Chemical Engineering Report Series
Kemian laitetekniikan raporttisarja No. 46
Espoo 2004

DEVELOPMENT OF VAPOUR LIQUID EQUILIBRIUM CALCULATION METHODS FOR CHEMICAL ENGINEERING DESIGN

Juha-Pekka Pokki

Dissertation for the degree of Doctor of Science in Technology to be presented with due permission for public examination and debate in Auditorium Ke 2 at Helsinki University of Technology (Espoo, Finland) on the 26th of November, 2004, at 12 noon.

Helsinki University of Technology
Department of Chemical Technology
Laboratory of Chemical Engineering and Plant Design

Teknillinen korkeakoulu
Kemian tekniikan osasto
Kemian laitetekniikan ja tehdassuunnittelun laboratorio

Distribution:
Helsinki University of Technology
Laboratory of Chemical Engineering and Plant Design
P. O. Box 6100
FIN-02015 HUT
Tel. + 358-9-4511
Fax. +358-9-451 2694
E-mail: Juha-Pekka.Pokki@hut.fi

ISBN 951-22-7377-2
ISSN 1236-875X

Otamedia Oy
Espoo 2004

Abstract

This thesis deals with the development of computational methods for vapour liquid equilibrium (VLE) and volumetric properties. The VLE in this thesis can be divided into the low- and medium-pressure VLE with an experimental part and into the high-pressure VLE with a modelling and simulation part. The volumetric properties in this thesis deal with the extension of the model for compressed liquid densities.

At low-pressure VLE, the emphasis was on the optimisation of model parameters. Two apparatus were built, a circulation still and an automated total pressure apparatus for the vapour liquid equilibrium measurements. The measurements were correlated with activity coefficient models for the liquid phase and with equations of state for the vapour phase. A program for correlating the vapour liquid equilibrium was developed. The measurements and VLE models optimised were needed in developing gasoline additives to replace methyl tertiary-butyl ether (MTBE).

At near-critical VLE, the emphasis was on the robustness of the VLE and simulation routines. There was a need for a simulator to find out the dynamics of several vessels and buffer tanks when vessels were in a runaway condition, exposed to fire and imbalance of flows, or all of these events simultaneously. In addition, the operation point near the VLE critical point was of special interest. A dynamic simulator where the vapour and liquid phases were assumed to be in equilibrium was developed. The pressure relieving devices were assumed to be the only devices to control the flow of material. The effect of the pipe network was not included in the simulator.

The temperature range of the model for the compressed liquid density of mixture was extended. The rigorous bubble point pressure and the critical point computed from the cubic equation of state were more consistent with the experimental data than the pseudo-bubble point and pseudo critical point of the original model. The application range of the model was extended at the expense of accuracy, but the extended model was better than a cubic equation of state.

Preface

The project for this thesis started in March 1999. Before 30.6.2000, the work was done partly at Helsinki University of Technology and partly at Neste Engineering Oy. The author thanks D.Sc. (Tech) Juhani Aittamaa and D.Sc. (Tech) Kari I. Keskinen at Neste Engineering Oy for building the bridge between university and industry and also for promoting the scholarships. The author acknowledges the scholarships from Foundation of Helsinki University of Technology and Research Foundation of Neste Oy. Professor Markku Hurme at Helsinki University of Technology is acknowledged for his supervision of my Licentiate Thesis and encouragement during this doctoral thesis.

After 1.7.2000 the project continued at Helsinki University of Technology as research on thermodynamics. The author thanks professor Juhani Aittamaa for the supervision of this thesis. The author also thanks TEKES (National Technology Agency of Finland) and five industry partners for funding the project on measurement of vapour liquid equilibrium. My colleagues and co-authors Petri Uusi-Kyyny, Marko Laakkonen, Younghun Kim, Piia Haimi, Minna Pakkanen, Tuomas Ouni, Matti Pasanen, Anna Zaytseva at our laboratory and professors Karel Řehák and Jaroslav Matouš in Prague, Czech Republic, are acknowledged for their ideas and contributions. The author thanks the staff at mechanical, electrical, and glass workshops of our department for the expertise in realising our drawings and ideas to apparatus and the co-author Raimo Multala for his expertise in automation systems.

D.Sc. (Tech) Mika Aalto is acknowledged for cooperation in density modelling and allowing access to the density database of his previous papers.

These three projects gave an opportunity to prepare the thesis so that it covers a wide range of temperature and pressure of fluid state. During the measurement project, my work as an assistant in teaching chemical engineering provided a good opportunity to apply the results of my thesis.

I thank my parents for encouraging my studies and this thesis. My wife Piia deserves thanks for her patience.

List of publications

[I] Uusi-Kyyny, P., Pokki, J-P., Aittamaa, J. & Liukkonen, S., (2001), Vapor Liquid Equilibrium for the Binary Systems of 2-Methyl-2-propanol + 2,4,4-Trimethyl-1-pentene at 333 K and 348 K and 2-Butanol + 2,4,4-Trimethyl-1-pentene at 360 K, *J. Chem. Eng. Data*, **46**, 686-691.

[II] Uusi-Kyyny, P., Pokki, J-P., Aittamaa, J. & Liukkonen, S., (2001), Vapor-Liquid Equilibrium for the Binary Systems of Methanol +2,4,4-Trimethyl-1-pentene at 331 K and 101 kPa and Methanol +2-Methoxy-2,4,4-trimethylpentane at 333 K, *J. Chem. Eng. Data*, **46**, 1244-1248.

[III] Pokki, J-P., Uusi-Kyyny, P, Aittamaa, J. & Liukkonen, S., (2002), Vapor-Liquid Equilibrium for the 2-Methylpentane + 2-Methyl-2-propanol and + 2-Butanol at 329 K, *J. Chem. Eng. Data*, **47**, 371-375.

[IV] Pokki, J-P., Řehák, K., Kim, Y., Matouš, J. & Aittamaa, J., (2003), Vapor-Liquid Equilibrium Data at 343 K and Excess Molar Enthalpy Data at 298 K for the Binary Systems of Ethanol + 2,4,4-Trimethyl-1-pentene and 2-Propanol + 2,4,4-Trimethyl-1-pentene*, J. Chem. Eng. Data*, **48**, 75-80.

[V] Uusi-Kyyny, P., Pokki, J-P., Laakkonen, M., Aittamaa, J. & Liukkonen, S., (2002), Vapor liquid equilibrium for the binary systems 2-methylpentane + 2-butanol at 329.2 K and n-hexane + 2-butanol at 329.2 and 393.2 K with a static apparatus, *Fluid Phase Equilib.*, **201**, 343-358.

[VI] Pokki, J-P., Laakkonen, M., Uusi-Kyyny, P. & Aittamaa, J., (2003), Vapour Liquid Equilibrium for the Cis-2-butene + Methanol, + Ethanol, + 2-Propanol, + 2-Butanol and + 2-Methyl-2-Propanol Systems at 337 K, *Fluid Phase Equilib.*, **212**, 129-141.

[VII] Uusi-Kyyny, P., Pokki, J-P., Aittamaa, J. & Multala, R., Vapour-Liquid Measurements with an Automated Static Total Pressure Apparatus, *20th European Symposium on Applied Thermodynamics*, Lahnstein near Koblenz, Germany, 9-12 October 2003.

[VIII] Pokki, J-P., Aittamaa, J. & Keskinen, K.I., (2000), Accuracy of Vapour - Liquid Critical Points Computed from Cubic Equations of State, *High Temperatures - High Pressures*, **32**, 449-459.

[IX] Pokki, J-P., Aittamaa, J., Keskinen, K.I. & Hurme, M., (1999), Modelling Emergency Relief for Processes at Near Critical Conditions, *Comp. Chem. Engng.* (*Suppl.*), **23**, S399-S402.

[X] Pokki, J-P., Aittamaa, J. & Hurme, M., (2001), Dynamic Simulation of the Behaviour of Pressure Relief Systems, *Comp. Chem. Engng.*, **25**, 793-798.

[XI] Pokki, J-P, Aalto, M. & Keskinen, K.I. (2002), Remarks on Computing the Density of Dense Fluids by Aalto-Keskinen Model, *Fluid Phase Equilib.* **194-197**, 337-351.

Authors contribution

[I] The author made the measurements together with co-author Uusi-Kyyny, took part in the interpretation of results, and writing the paper.

[II] The author made the measurements together with co-author Uusi-Kyyny, modified the computer code to calculate the results, and took part in writing the paper.

[III] The author made the measurements together with co-author Uusi-Kyyny, calculated the results, and wrote the paper.

[IV] The author programmed the computer code to compute excess enthalpy, calculated the results, and wrote the paper.

[V] The author developed the computer code to calculate the results, calculated the results, and took part in writing the paper.

[VI] The author developed the computer code to calculate the results, calculated the results, and wrote the paper.

[VII] The author took part in the design of automation and programmed the logical operations for the automation system.

[VIII - X] The author developed the model and the computer code, calculated the results, and wrote the paper.

[XI] The idea was developed together. The author programmed the computer code, calculated the results, and wrote the paper.

Table of contents

Notation

A	area of the consistency test
A_i	coefficient of Clausius-Clapeyron equation
$\boldsymbol{a}$	vector of coefficients of the spline
B_i	coefficient of Clausius-Clapeyron equation
$\boldsymbol{b}$	vector of coefficients of the spline
$\boldsymbol{C}$	vector of function values of the spline
$\boldsymbol{c}$	vector of coefficients of the spline
$\boldsymbol{d}$	vector of coefficients of the spline
f_i	function
g	Rachford-Rice function
h^M	enthalpy change of mixing
H^E	excess enthalpy
h	enthalpy
I_i	criteria in consistency test
$\boldsymbol{J}$	Jacobian matrix
j_{ij}	element of the Jacobian matrix
K_i	vapour liquid equilibrium factor
k_i	coefficient in consistency test
m	mass
n	amount of moles
p	pressure
$\boldsymbol{p}$	vector of points of the spline
Q	flow of energy
R	gas constant or
$\boldsymbol{R}$	approximate correlation coefficient matrix
r_i	reaction rate of component i
r_{ij}	element of approximate correlation coefficient matrix
T	temperature
t_v	statictical t-distribution value
t	parameter of the spline or time
U	internal energy
V	volume
v^M	volume change of mixing
$\boldsymbol{w}$	trial vapour or liquid phase
x_i	mole fraction of component i in liquid phase
y_i	mole fraction of component i in vapour phase
z_i	total mole fraction of component i

greek

α	internal variable
β	vapour fraction
ε	derivative in consistency test
ω	acentric factor
γ	activity coefficient
θ	parameter

σ	variance
ϕ	fugacity coefficient

superscripts and subscripts

c	critical
CAT	catalyst, solid
i,j	component
k	parameter
l	liquid
lt	liquid trial phase
max	maximum
min	minimum
POL	polymer, solid
RCT	reactor
spec	specified
TOT	total amount
v	vapour
vt	vapour trial phase

abbreviations

AARE	average absolute relative error
AAD	average absolute deviation
MTBE	methyl tertiary-butyl ether
tm	modified tangent plane distance
VLE	vapour liquid equilibrium
LLE	liquid liquid equilibrium

1 Measurement of low and medium pressure vapour liquid equilibrium

The experimental part of this thesis deals with the measurement of vapour liquid equilibrium. The measurement of the low-pressure (below and at atmospheric pressure) vapour liquid equilibrium is reported in papers [I] – [IV] and the measurement of the medium-pressure (below atmospheric to 20 bars) vapour liquid equilibrium in papers [V] – [VII].

1.1 Total pressure apparatus

During the past decades, the technique of total pressure measurement has been reported in several publications. In the pioneering work of Gibbs and van Ness (1972), the total pressure technique was developed by employing syringe pumps. Previously, the degassed components were distilled directly into the test cell. After each experiment, the cell was emptied and evacuated. Gibbs and van Ness (1972) degassed the components by freezing and thawing and led the components into the syringe pumps. The subsequent injections formed the desired composition into the test cell. Ronc and Ratcliff (1976) developed the design of Gibbs and van Ness by measuring the temperature inside the cell and employing a pressure meter with a wider temperature range. Compared to Gibbs and van Ness (1972) and Ronc and Ratcliff (1976), Mentzer et al. (1982) constructed the cell from stainless steel with a copper gasket between the cell body and the lid to make it more leak-proof. Mentzer et al. (1982) also improved the mixing by entering the pure liquids through the sides of the cell rather than through the top of the cell.
Kolbe and Gmehling (1985) used a glass cell and a stainless steel lid. The apparatus of Rarey and Gmehling (1993) seems to be the first automated total pressure apparatus. The pressure was measured as a differential pressure between the equilibrium cell and reference cell.

Building a total pressure apparatus at our laboratory started in autumn 2000, because there was an industrial need for vapour liquid equilibrium measurements. The measurements are used in developing processes to replace MTBE in gasoline, [I] – [VI].

1.1.1 Apparatus

The total pressure apparatus of our laboratory is presented in [V]. The equilibrium cell was made of AISI 316L steel and its volume was determined accurately every time it was modified. The volume of the cell was determined by injection of distilled water in constant temperature and defined pressure. The accurate volume is reported in the publications [V] – [VII]. The equilibrium cell was immersed in a large, appr. 70 dm^3 water bath. The large water bath was well mixed with a propeller and thermostated with a heating coil where water flowed inside. The water flow inside the heating coil was thermostated with a Lauda Ecoline RE206 water bath. The stability of the large water bath is discussed in [V].

The equilibrium cell temperature was measured with a temperature probe that was located in contact with the equilibrium cell wall. The temperature meter Systemteknik S2541, (Frontec) equipped with Pt-100 probes was calibrated at the Finnish National Standards Laboratory. The resolution of the temperature measurement system was 0.005 K and the calibration uncertainty was ±0.015 K. The uncertainty in the temperature measurement system was estimated to be ±0.02 K.

The pressure measurement line from the cell to the pressure transducer was electrically traced to avoid condensation. The pressure was measured with a Digiquartz 2100A-101-CE pressure transducer (0-689 kPa, compensated temperature range 219-380 K) equipped with a Digiquartz 740 intelligent display unit. The uncertainty of the pressure measurement was ±0.069 kPa according to data provided by the manufacturers of the pressure measurement devices. The pressure measurement system was checked against a DHPPC-2 pressure calibrator and also the temperature compensation of the pressure transducer was checked. The accuracy of the pressure calibrator was 0.3 kPa, which is worse than the stated accuracy of the pressure transducer used.

Injections of the components were made with syringe pumps (Isco 260 D and Isco 100 DM). The temperatures of the barrels of the syringe pumps were controlled. The temperatures of the syringe pumps were measured with temperature probes located in contact with the syringe pump barrels. The volumes of the cylinder of the pumps were calibrated gravimetrically with water injections in the beginning of the project.

1.1.2 Procedure of measurement

Degassed components were loaded into evacuated piston pumps. After the evacuation of the cell and the feed lines, the components were injected into the cell of known volume in a certain order. The first component was injected into the cell and equilibrated for 20 minutes. The unchanged vapour pressure after the second addition and the equilibration of the first component indicated the success of degassing. The second component was added in several portions until the cell was nearly full. The cell was evacuated and the second component was added in two portions to indicate the success of degassing of the second component. Next the first component was added in several portions until the cell was nearly full. The displacement of the piston pumps, pressure and temperature of the pumps, system pressure, and system temperature were measured. The number of moles injected was calculated from the displacement of the piston and density of the component at the pump temperature and pump pressure. The measurement of the isotherm was successful, if the both sides of the isotherm met at the centre of the mole fraction space.

The vapour and liquid composition were computed when also the pure component vapour pressure and the saturated liquid molar volume at system pressure were known. The measurement was isothermal with very small fluctuation of temperature; the fluctuation was approximately 0.05 K. The isothermal measurement is not necessary from the data reduction point of view but it was done to evaluate the success of the measurement. The consistency of total pressure measurements could not be checked because the liquid and vapour mole fraction is back-calculated using the equations the consistency test would use.

1.1.3 Automation of apparatus

Since publications [V] and [VI], the apparatus have been automated to reduce the labour involved in the measurements significantly. This increased the measurement capacity of the apparatus. However, it did not remove the supporting activities such as cleaning, evacuation, and degassing.

The measurements were read via RS232 ports. There were three temperature measurements that were read from a Systemteknik S2541 temperature meter: the temperature of the large water bath and the temperatures of two syringe pumps. The equilibrium cell was immersed in a large 70 dm^3 water bath that was heated with a Lauda Ecoline RE206. The set point of the Lauda water bath was set via RS232 ports. The pressure was measured with a Digiquartz 2100A-101-CE pressure transducer (0-689 kPa) and read via RS232 ports.

The valves attached to the lid of the equilibrium cell were operated with Vexta stepping motors equipped with gearboxes. The interface cards connected the stepping motors to the PC via RS232 ports. The syringe pumps Isco 260 D and Isco 100 DM were connected to computer via RS232 ports. The syringe pumps injected the components into the equilibrium cell and the pumped volumes were recorded. The pumps were operated in a constant pressure mode. The stepping motor opened the valve and the syringe pump injected the component into the cell until the target volume of the pump was reached and then the valve was closed. The pump operated until the set point of the constant pressure was reached. The amount of injected moles was computed from the displacement of the piston of the pump. The equilibration time for one experimental point of this system was found to be less than 20 minutes. The data between these seven devices and the PC was transferred via Smartio C168H / 8 RS232 ports card at PCI bus. Data collection also allowed a detailed analysis of the measurements and further calculation of final results.

The flow diagram of the automated apparatus is presented in Figure 1.1. It was operated in Windows NT4 environment on a PC, where the controlling program was Wonderware InTouch. The program used so-called condition scripts, that is, the loop was running continuously and if the condition was true, an action was taken. The drawback of this program was that it did not accept subprograms or vectors.

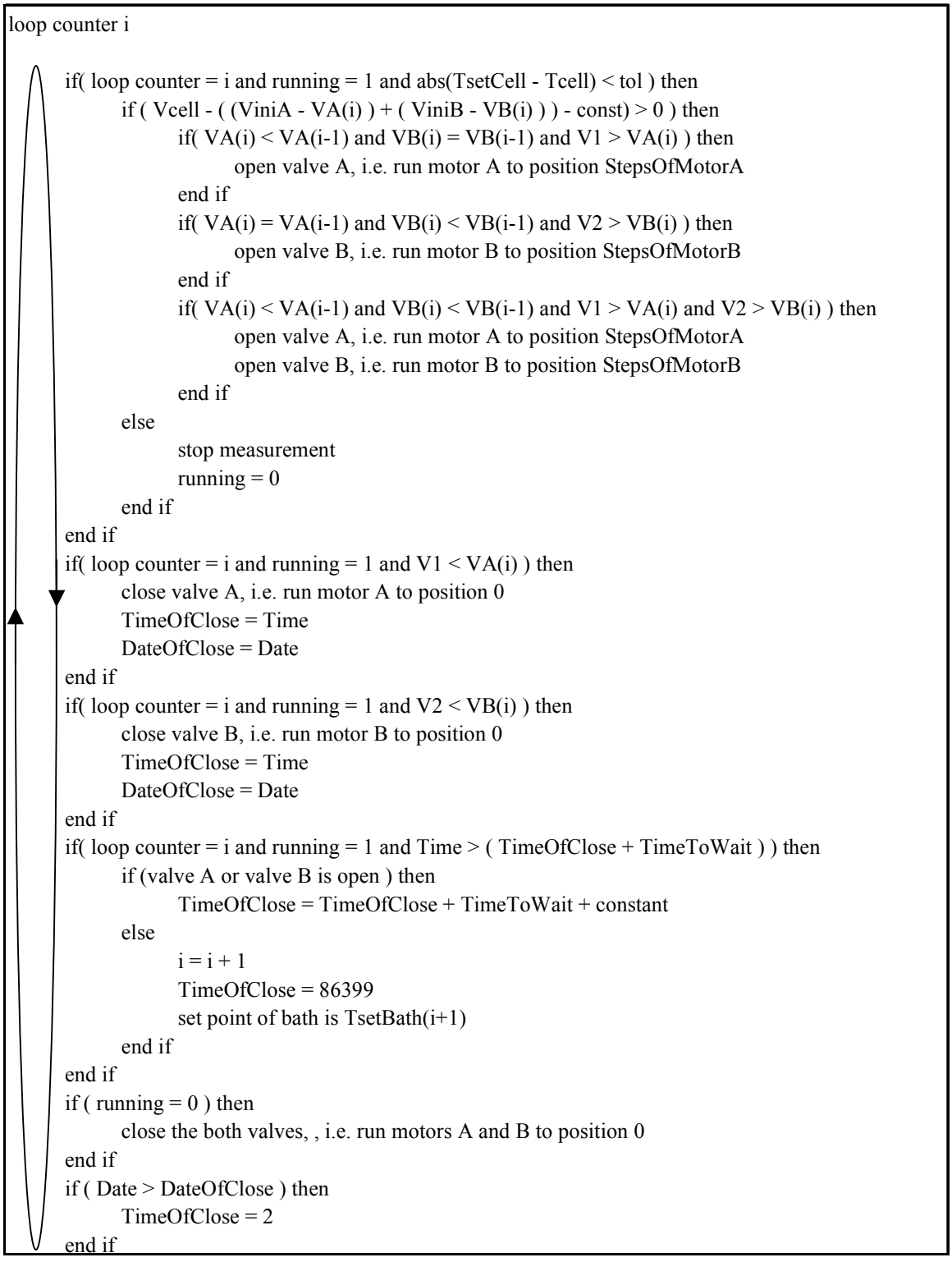

Figure 1.1. *Operation logic of the automated total pressure apparatus. Variables are presented as vectors to compress the presentation, but vectors are not available in Wonderware InTouch. V1 and V2 are the volumes of the syringe pumps A and B at any moment of time, and VA(i) and VB(i) are the target volumes of pumps A and B.*

1.2 Total pressure measurements, calculation of phase composition

The pure component vapour pressure was measured when the pure component was injected into the cell. This value was used in [V] and [VI] but the later articles [VII] used the corrected value. The bath temperature fluctuates approximately ±0.05 K during the measurement. Because the pure component vapour pressure affects the vapour liquid equilibrium very much, the vapour pressure was corrected to increase the accuracy.

$$p_{i,k}^{0} = p_{i,pure}^{0} + \left(\frac{dp_{i,pure}^{0}}{dT} \right)\left(T_k - T_{i,pure}\right) \qquad (1.1)$$

The derivative was computed from the vapour pressure correlation at the pure component temperature. It is important to use the measured vapour pressure of pure component in data reduction. If the vapour pressure of a pure component is not matching exactly the system pressure at $x_1 = 0$ and $x_2 = 1$, the activity coefficient model tries to compensate the error in vapour pressure of the pure component and the accuracy of modelling decreases.

Because the vapour and the liquid mole fractions were not analysed, they must be calculated with a specific method. The method proposed by Barker (1953) was used to convert the moles of each component injected into the cell to mole fraction of the vapour and liquid phase. It is based on phase equilibrium and volume balance. The Barker method can be applied to both the $\phi - \phi$ (fi-fi) approach and to the $\gamma - \phi$ (gamma-fi) approach. In this thesis, only the $\gamma - \phi$ (gamma-fi) approach was used in data reduction, because activity coefficient models give better accuracy than equation of state models. The fugacity of a saturated pure component at measured temperature was calculated once from the SRK, Soave (1972), equation of state. Initially, it was assumed that the liquid mole fraction was equal to the total mole fraction, the fugacity of component *i* in vapour phase was unity, and the volume of the vapour phase followed the ideal gas law. With these assumptions, the bubble point pressure was calculated. The difference between the calculated and measured pressure was minimised by optimising the coefficients of the activity coefficient model. By assuming the ideal volume of the liquid phase, the amount of moles in the vapour phase was solved from the volume balance. The calculation of mole fraction of the vapour phase made it possible to solve the amount of moles of individual components in the vapour phase and in the liquid phase. Next the mole fraction of the liquid phase was updated and a new iteration loop started. After the first loop, the fugacity of component *i* in the vapour phase and the vapour molar volume was updated from the SRK equation of state. The iteration was continued until the change in the amount of moles of individual component in the liquid phase was below tolerance. The mathematics of Barker data reduction is presented in [V] and an error analysis is presented in [VI].

The vapour phase correction is small at low to moderate pressure and for systems not having very a high or low relative volatility. The calculated mole fraction of the liquid phase can be regarded as measured liquid mole fraction.

The saturated liquid molar volume was not measured but computed from the correlation. According to Daubert and Danner (1989), these correlations are accurate and the error associated in them is less than 1 %. This usually causes a smaller error than the omission of excess molar volume. The omission of excess molar volume causes an error in VLE data reduction. The closer to critical point, the larger the error is. The effect of the EOS binary interaction parameter on the fugacity coefficient of component *i* in vapour phase is minimal. The pressure is relatively low and the system is far from the critical point. In addition, the activity coefficient model compensates the differences between models of equations of state during the Barker data reduction.

The objective function was the absolute error or the absolute relative error in pressure. The target of optimisation was to decrease the modelling error in the system pressure to be smaller than the error in the pressure measurement. The most suitable model was the Legendre polynomial, Gmehling and Onken (1977), because of its high accuracy and flexibility. In principle, any activity coefficient model, as long as it gives sufficient accuracy, can be used in Barker data reduction.

The thermodynamic consistency cannot be checked for the total pressure data because the reduction of total pressure data is based on the Gibbs-Duhem equation used in consistency tests. A comparison of the pure component vapour pressure to literature references and matching the both sides of the isotherm at the centre of the mole fraction range indicate the success of the measurement.

Munjal et al. (1983) compared the reduction methods of total pressure measurements, namely the Barker (1953) and Mixon et al. (1965) methods. The drawback of the Barker method is its a priori assumption on the particular model on activity coefficients and its parameters. It is difficult to take into account the unusual behaviour of total pressure at the end points of the mole fraction space in the model, because the weight of the end points is small compared to the whole range. The conclusion of Munjan et al. (1983) was that the Barker method is not at best at end points of composition range. In addition, Plank et al. (1981) emphasised that the activity coefficients at infinite dilution reflect the parameters of the particular model and may not reflect the true behaviour at infinite dilution.

Munjan et al. (1983) concluded that the drawback of the Mixon et al. method is the obviously erroneous values of activity coefficients at the end points of mole fraction space if experimental pressure has some scatter and the splined fits are forced to follow that scatter too strictly. According to Plank et al. (1981) splined fits are not involved in the Mixon et al. method itself, but they are needed to interpolate the pressure versus mole fraction to get evenly spaced values for the finite-difference iteration. Too strict splined fits in the scattered data lead to poor behaviour of the first and second derivatives, and these are reflected in the abnormal behaviour of activity coefficient plots. Both Plank et al. (1981) and Munjan et al. (1983) claimed the Mixon et al. method to be more accurate compared to the Barker method.

We selected the Barker method for the data reduction because it gives higher reliability of activity coefficients than the Mixon et al. method and the Barker method smoothes out the measurements in a consistent way. We also report the number of injected moles and all other details for those who want to reduce the data with the methods they prefer.

1.3 Recirculation still

According to Raal and Mühlbauer (1998) the dynamic equilibrium stills are the earliest types of apparatus and account for the large portion of published VLE measurements. The circulation of the vapour phase only or the circulation of both the vapour and the liquid phases of the boiling mixture is the principle of operation.

The Othmer (1928) apparatus circulated only the vapour phase. According to Raal and Mühlbauer (1998), it had some deficiencies such as the location of temperature probe, the hold-up of condensate receiver was large, partial condensation of vapour on the wall of boiling flask, and flashing of vapour rich in the more volatile component.

The Gillespie (1946) apparatus circulated both the vapour and liquid phase. It applied the Cottrell pump and was the first to return the liquid to the boiling chamber. A Cottrell pump is a narrow tube where the force of the boiling liquid pumps the two-phase vapour liquid mixture upwards. According to Raal and Mühlbauer (1998) the setup of Gillespie (1946) had some problems; the condensed vapour sample and the liquid sample were not in equilibrium, partial condensation was possible at the temperature well, sampling interrupted the operation, and the mass transfer in the Cottrell pump was not satisfactory because of the short contact time.

The Yerazunis (1964) apparatus circulated both the vapour and the liquid phase. Its novel feature compared to earlier apparatus was the co-current flow of vapour-liquid mixture in the packed equilibrium chamber. Furthermore, sampling valves that interrupted the operation were replaced with sampling chambers with built-in septa. They operated well except for high vacuum.

Building a recirculation still at our laboratory started in winter 2000. The apparatus was made of glass in the workshop of our department. The set up was Yerazunis type with small modifications suggested by professor Matous from the Czech Republic. The apparatus was built very quickly compared to our total pressure apparatus. It made possible to respond quite rapidly to the industrial need for vapour liquid equilibrium measurements. [I] – [VI].

1.3.1 Apparatus

The recirculation still of our laboratory is presented in [I] – [IV]. It allowed isothermal or isobaric measurements at lower than or equal to atmospheric pressure. The apparatus was tested by measuring the vapour pressure of water and by measuring the isobaric system of *n*-heptane + toluene at 1 atm. Results compared well with literature data.

The liquid volume in the boiling chamber was approximately 80 cm^3. The Pt-100 probe was located at the bottom of the packed section of the equilibrium chamber in a thermometer well. For temperature measurements, two temperature meters were used. Only one of them was in operation during measurements.

One was a Thermolyzer S2541 (Frontec) temperature meter with a Pt-100 probe calibrated at the Finnish National Standards Laboratory. The resolution of the temperature measurement system was 0.005 K and the calibration uncertainty was ±0.015 K.

The other was an Ametek DTI100 temperature meter with a Pt-100 probe calibrated at the Inspecta Oy (Accredited Calibration Laboratory). The resolution of the temperature measurement system was 0.01 K and the calibration uncertainty was ±0.05 K.

The uncertainty in the temperature measurement, estimated to be between ±0.05 K and ±0.07 K, was mostly due to fine-tuning of pressure at a measured isotherm. At atmospheric measurements, the uncertainty in temperature is smaller due to relatively slow changes in atmospheric pressure.

The pressure was measured with a Druck pressure transducer (0-100 kPa) equipped with a Red Lion panel meter. The uncertainty of the pressure measurement was ± 0.07 kPa according to the data provided by the manufacturer of the pressure measurement devices. The pressure measurement system was calibrated against a DHPPC-2 pressure calibrator. Including the calibration uncertainty, the uncertainty in the pressure measurement system is ± 0.15 kPa.

1.3.2 Procedure of measurement

The vapour pressure of the first pure component was measured first. After adding the second component, the equilibration took approximately 30 minutes. Both the condensed and the cooled vapour phase and the cooled liquid phase samples were analysed. Temperature and pressure were read at the same time as the samples were withdrawn. The addition of the second component continued most of the mole fraction range, if some mixture rich in the first component was taken away. However, at the end of the isotherm or isobar the apparatus was emptied and evacuated. The vapour pressure of the second component was measured. The additions of the first component were continued until the other side of the isotherm or isobar was met. In this work, the samples were analysed using a gas chromatograph. It requires the calibration mixtures to prepare the response factors. The mole fraction of the sample was back-calculated from the peak areas and response factors.

1.3.3 Consistency tests

The quality of measurements made by the recirculation apparatus can be checked by consistency tests based on thermodynamic relations. These tests are an integral test, an infinite dilution test and a point test. The results of these tests can be seen in the tables and figures of article [I]. Later articles [II], [III] and [IV], which were published during this project, only summarise the results in tables and show only the figure for the point test.

1.3.3.1 Area test

According to Kojima et al. (1990) and Gmehling and Onken (1977), the idea of the area test is to calculate the value of the integral between mole fractions from 0 to 1. The closer to zero the area is, the better the measurement is.

$$A = 100\left|\int_0^1 \ln\left(\frac{\gamma_1}{\gamma_2}\right)dx_1 + \int_0^1 \varepsilon \cdot dx_1\right| \tag{1.2}$$

where

$$\varepsilon = \left(\frac{-h^M}{RT^2}\right)\left(\frac{dT}{dx_1}\right) \tag{1.3}$$

for isobaric data and

$$\varepsilon = \left(\frac{v^M}{RT}\right)\left(\frac{dp}{dx_1}\right) \tag{1.4}$$

for isothermal data.

According to Smith et al. (1996), the enthalpy of mixing h^{M} is equal to excess enthalpy H^{E} and volume change of mixing v^{M} is equal to excess volume V^{E}.

Kojima et al. (1990) suggested calculating $\frac{dT}{dx_1}$ from the equation

$$\Delta T = \frac{x_1 x_2}{a' + b'(x_1 - x_2) + c'(x_1 - x_2)^2} \tag{1.5}$$

where

$$\Delta T = T - x_1 T_1 - x_2 T_2 \tag{1.6}$$

then

$$\frac{dT}{dx_1} = \frac{d\Delta T}{dx_1} + T_1 - T_2 \tag{1.7}$$

In addition to that the enthalpy of mixing is correlated

$$h^M = x_1 x_2 \left[k_0 + k_1(x_1 - x_2) + k_2(x_1 - x_2)^2 + \ldots\right] \tag{1.8}$$

where

$$k_i = k_{T0,i} + k_{T1,i}/T \tag{1.9}$$

According to Raal and Mühlbauer (1998) and Gmehling and Onken (1977), the drawbacks of the integral test are as follows: compensating errors in the ratio of activity coefficients may cause inconsistent measurements to pass the test, isobaric data requires excess enthalpy data, the area test does not check individual points, and the measured pressure cancels in the ratio of activity coefficients. Pressure as an accurate and easily measurable variable disappears in the ratio of activity coefficients, but pressure affects only the fugacity coefficients.

1.3.3.2 Infinite dilution test

The purpose of the infinite dilution test is to check consistency at the dilute range. According to Kojima et al. (1990), the function of excess Gibbs energy and ratio of activity coefficients should coincide at the end points of the mole fraction range. The better the coincidence is, the better the measurement is.

$$I_1 = 100 \left| \frac{\left(\frac{g^E / RT}{x_1 x_2} \right)_{x1=0} - \ln\left(\frac{\gamma_1}{\gamma_2} \right)_{x1=0}}{\ln\left(\frac{\gamma_1}{\gamma_2} \right)_{x1=0}} \right| \qquad (1.10)$$

$$I_2 = 100 \left| \frac{\left(\frac{g^E / RT}{x_1 x_2} \right)_{x2=0} - \ln\left(\frac{\gamma_2}{\gamma_1} \right)_{x2=0}}{\ln\left(\frac{\gamma_2}{\gamma_1} \right)_{x2=0}} \right| \qquad (1.11)$$

1.3.3.3 Point test

Gmehling and Onken (1977) used a test where the difference between the modelled and measured pressure is minimised and then the difference between the modelled and measured vapour mole fraction of individual measurements serves as a criterium for the passing of the test. This test is not at best for components where the separation factor is bigger than 10 or very close to unity and the boiling point difference is very large. In those cases the vapour fraction of more volatile component is close to unity over large range of mole fraction.

Raal and Mühlbauer (1998) presented several consistency tests used in testing the measurements. It should be remembered that testing of consistency does not make the measurement any better. It only reveals some errors done during the measurement. Once the consistency is tested, the optimisation of model parameters is required. The objective function is not limited to pressure only as it is in the case of total pressure measurements, but measurements made with recirculation still give some more objective functions; difference in vapour composition, difference in activity coefficients and difference in temperature.

1.4 Molar excess enthalpy

1.4.1 Measurements

The systems reported in paper [IV] were measured at the Department of Physical Chemistry, Institute of Chemical Technology, Prague, Czech Republic, by the group of professor Jaroslav Matous.

1.4.2 Limitations of excess enthalpy modelling

The excess enthalpy can be computed as a derivative of logarithm of activity coefficients with respect to temperature. The activity coefficient model requires the dependence of temperature to be suitable for excess enthalpy modelling. One serious problem with these models is their limited ability to represent large numerical values of excess enthalpy. According to Christensen (1984) the Wilson (1963) and NRTL, Renon and Prausnitz (1968), models in their original form break down for $\left|H^E\right| >\approx 840$ J/mol and the UNIQUAC model breaks down for $\left|H^E\right| >\approx 1000$ J/mol. By expressing the coefficients of the activity coefficient model with polynomials of temperature, the dependence can be enhanced. Among the first to propose the extended temperature dependence were Assilineau and Renon (1970). They modified the parameters (g_{12}-g_{11}), (g_{21}-g_{22}) and α_{12} of the NRTL activity coefficient model by adding linear temperature dependence. Modifications of correlative models are summarised by Christensen et al. (1988).

The temperature dependence is also added in the predictive model UNIFAC. The benefit of Dortmund modified UNIFAC (Weidlich and Gmehling (1987)) and Lyngby modified UNIFAC (Larsen et al. (1987)) compared to the original UNIFAC (Fredenslund et al. (1977)) is the increased temperature dependence. These modified UNIFAC models can predict VLE, liquid-liquid equilibrium (LLE) and excess enthalpy better than the original model.

1.5 Optimisation of activity coefficient model parameters

The discussion of the optimisation of parameters in [I]-[VII] is extended by the sensitivity of the parameters. The parameters of the activity coefficient model are optimised and reported in each paper. The optimisation methods were Nelder-Mead's extended Simplex, Fredenslund et al. (1977), and Davidon (1975). In many textbooks, such as Constantinides and Mostoufi (1999) and Cutlip and Shacham (1999), the theory of the sensitivity of parameters is for linear models. Rose (1981) discussed the application of the linear theory for the non-linear models. This approach gives the approximate confidence level and approximate correlation coefficient matrix. For the non-linear models, the Jacobian matrix is computed

$$\boldsymbol{J} = \begin{bmatrix} \frac{\partial f_1}{\partial \theta_1} & \cdots & \frac{\partial f_1}{\partial \theta_k} \\ \vdots & \cdots & \vdots \\ \frac{\partial f_n}{\partial \theta_1} & \cdots & \frac{\partial f_n}{\partial \theta_k} \end{bmatrix} \tag{1.12}$$

where f_i is the objective function of the single measurement and θ_k is the value of the parameter. The derivatives are dependent on the model and on the values of the parameters θ_k. The Jacobian is computed numerically, because Simplex does not

need it. According to Cutlip and Shacham (1999), for the linear model, and when applied to this non-linear case, the value of the parameter is between

$$\theta_i - \sqrt{j_{ii}\sigma}t_k \le \theta_k \le \theta_k + \sqrt{j_{ii}\sigma}t_v \qquad (1.13)$$

where j_{ii} is the diagonal elements of $\left(\boldsymbol{J}^T\boldsymbol{J}\right)^{-1}$, σ is the variance and t_v is the statistical t-distribution value corresponding to the degrees of freedom at *v* confidence level. The confidence level was 95 % in this work. Shacham and Brauner (1997) explained that large confidence intervals indicate that a small change in data can cause large changes in the parameter values. When the parameter value $\theta_k = 0$ is included in the confidence range, there is no statistical justification to include the parameter into the model.

The correlation coefficient matrix $\boldsymbol{R}$ for the linear model is according to Constantinides and Mostoufi (1999), and when applied to this non-linear case the elements of the matrix $\boldsymbol{R}$ are

$$r_{ij} = \frac{j_{ij}}{\sqrt{j_{ii}\,j_{jj}}} \qquad (1.14)$$

The elements have their value in the range of $-1.0 \le r_{ij} \le 1.0$. The value of the off-diagonal element should be close to zero to have a low correlation between parameters. A complete correlation, $\left|r_{ij}\right| = 1.0$, between the parameters tells that a change in the value of one parameter can be completely compensated by a change in the other parameter.

1.5.1 Example: Data reduction of Barker's method

The total pressure measurement of binary mixture *n*-hexane + 2-butanol at 329 K is presented as an example. The number of parameters was increased from 1 to 5 during the steps of optimisation of Legendre parameters. The Legendre polynomial used is presented in Gmehling and Onken (1977). The average absolute deviation (AAD), the average absolute relative error (AARE), the parameters, their approximate confidence limits and approximate correlation coefficient matrix are presented in Table 1.1.

Table 1.1 *Approximate confidence limits and correlation coefficient matrix for system n-hexane + 2-butanol with various number of Legendre parameters*

	1 parameter			AAD / kPa	AARE / %			
	The appr. confidence limits			0.207	0.39			
k	$a_{k,0}$	conf. limit	%					
1	1.66190	0.00658	0.4					
	2 parameters			AAD / kPa	AARE / %			
	The appr. confidence limits			0.132	0.25			
k	$a_{k,0}$	conf. limit	%	The appr. correlation coefficient matrix.				
1	1.66395	0.00328	0.2	1	-0.325			
2	0.33463	0.00700	2.1	-0.325	1			
	3 parameters			AAD / kPa	AARE / %			
	The appr. confidence limits			0.123	0.24			
k	$a_{k,0}$	conf. limit	%	The appr. correlation coefficient matrix.				
1	1.66823	0.00462	0.3	1	-0.129	0.608		
2	0.33042	0.00712	2.2	-0.129	1	0.281		
3	0.22014	0.00706	3.2	0.608	0.281	1		
	4 parameters			AAD / kPa	AARE / %			
	The appr. confidence limits			0.094	0.15			
k	$a_{k,0}$	conf. limit	%	The appr. correlation coefficient matrix.				
1	1.66952	0.01491	0.9	1	-0.842	0.724	-0.501	
2	0.36109	0.02991	8.3	-0.842	1	-0.754	0.842	
3	0.23577	0.01803	7.6	0.724	-0.754	1	-0.706	
4	0.08194	0.01710	20.9	-0.501	0.842	-0.706	1	
	5 parameters			AAD / kPa	AARE / %			
	The appr. confidence limits			0.087	0.13			
k	$a_{k,0}$	conf. limit	%	The appr. correlation coefficient matrix.				
1	1.66584	0.05915	3.6	1	-0.959	0.709	-0.632	0.448
2	0.35270	0.10251	29.1	-0.959	1	-0.843	0.813	-0.581
3	0.21948	0.08871	40.4	0.709	-0.843	1	-0.963	0.899
4	0.06943	0.05286	76.1	-0.632	0.813	-0.963	1	-0.835
5	0.01642	0.02736	166.6	0.448	-0.581	0.899	-0.835	1

Table 1.1 shows the decrease in the AAD and the AARE when the number of coefficients increased. The decrease in the AAD was minor when the number of parameters changed from four to five. The confidence limits of the parameters increased and the absolute values of the off-diagonal elements become closer to the unity. In addition the confidence limit of the fifth parameter included the parameter value zero. In that sense the four parameters were sufficient but there was a small improvement in AAD and AARE when the five parameters were optimised. The

graphical presentation of the pressure deviation as a function of total mole fraction is presented in Figure 1.1.

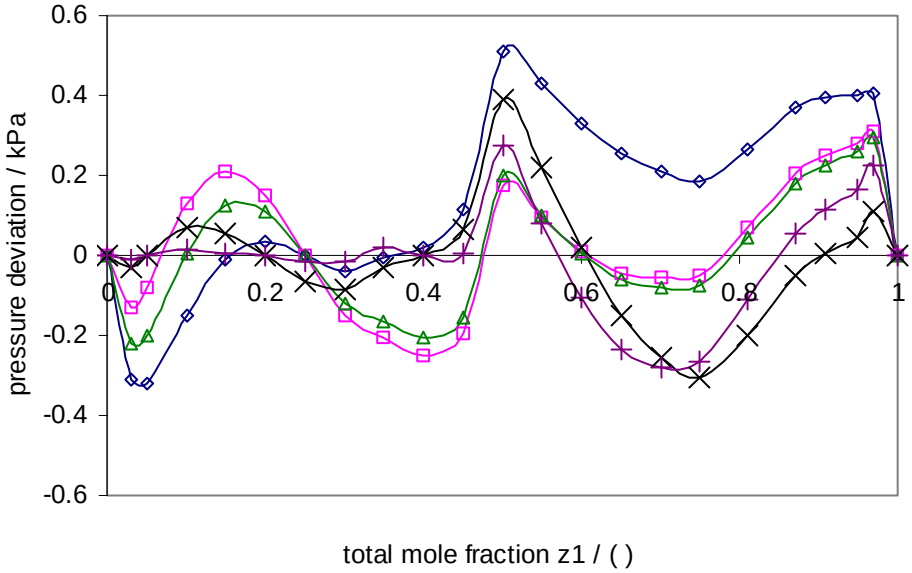

Figure 1.1 *Decrease of the deviation in pressure as the number of Legendre parameters increase. ◇, 1 parameter; □, 2 parameters; △, 3 parameters; ×, 4 parameters; +, 5 parameters*

Figure 1.2 gives the graphical presentation on how the average absolute deviation (AAD) and the average absolute relative error (AARE) decrease as the number of parameters increases.

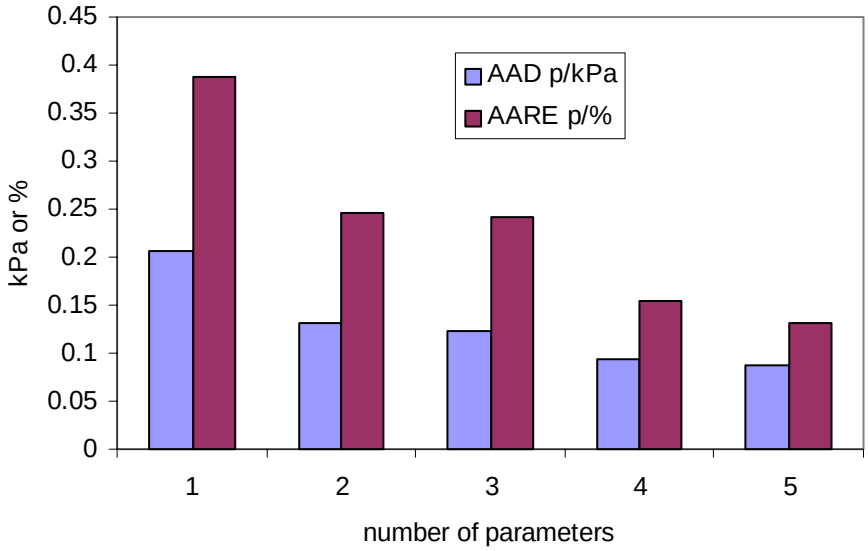

Figure 1.2 *Decrease of the average absolute deviation and average absolute relative error in pressure as the number of Legendre parameters increase*

1.5.2 Example: VLE and H^E measurements

Parameters of the Wilson (1964) model were optimised for ethanol + 2,4,4-trimethyl-1-pentene. The measurements were reported in [IV] and Uusi-Kyyny et al. (2003). In this example VLE at 1 atm, VLE at 343 K, H^E at 298 K separately and all VLE and H^E data together were used in the optimisation of parameters. The optimised parameters, their approximate confidence limits at 95 % level, the value of the parameters at the lower and the upper limit and approximate correlation coefficient matrix are presented in Table 1.2.

Table 1.2 *Approximate confidence limits and approximate correlation coefficient matrix for system ethanol + 2,4,4-trimethyl-1-pentene with different objective function and set of measurements*

VLE at 1 atm					
a_{ij}	conf. limit	low limit a_{ij}	high limit a_{ij}	The appr. correlation coefficient matrix.	
7640.9	106.4	7534.4	7747.3	1	-0.801
975.6	87.6	888.0	1063.2	-0.801	1
AARE in T/%		0.02			
VLE at 343 K					
a_{ij}	conf. limit	low limit a_{ij}	high limit a_{ij}	The appr. correlation coefficient matrix.	
8176.2	74.9	8101.3	8251.0	1	-0.798
687.2	51.5	635.7	738.7	-0.798	1
AARE in p/%		0.25			
HE at 298 K					
a_{ij}	conf. limit	low limit a_{ij}	high limit a_{ij}	The appr. correlation coefficient matrix.	
6395.9	113.9	6282.0	6509.8	1	0.930
1527.3	81.1	1446.2	1608.4	0.930	1
AARE in HE/%		2.91			
VLE at 1 atm, 343 K and HE at 298 K					
a_{ij}	conf. limit	low limit a_{ij}	high limit a_{ij}	The appr. correlation coefficient matrix.	
6582.6	110.7	6471.8	6693.3	1	0.538
1661.3	91.2	1570.1	1752.5	0.538	1
AARE in T/%		0.12			
AARE in p/%		2.04			
AARE in HE/%		3.28			

The confidence limits are narrow and the absolute value of the off-diagonal elements is not close to unity. The parameters are presented graphically in Figure 1.3

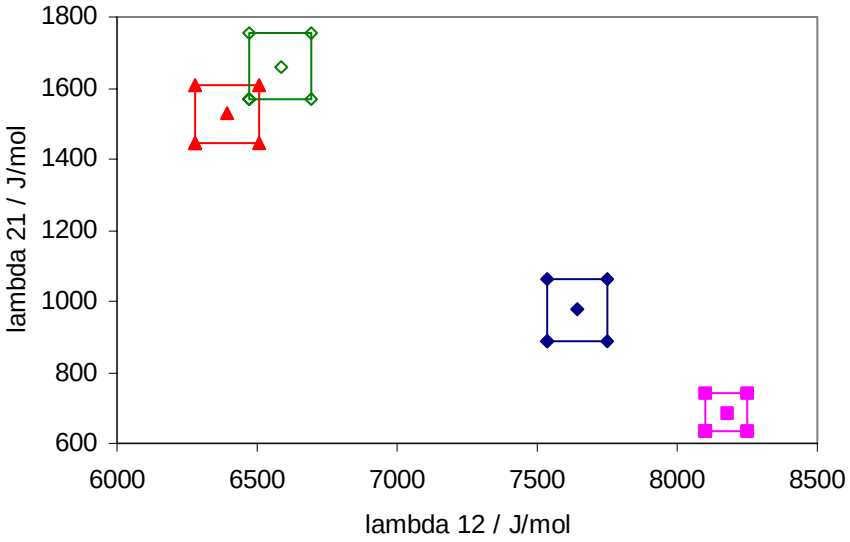

Figure 1.3 *Value of parameter and individual confidence intervals, system ethanol + 2,4,4-trimethyl-1-pentene and Wilson model.* ◆, *VLE at 1 atm ;* ■, *VLE at 343 K;* ▲, H^E *at 298 K;* ◇, *VLE at 1 atm, 343 K and* H^E *at 298 K together.*

It can be seen that the optimal values hit at different regions of the parameter space. The effect of the values of the parameters was studied with the following combinations. The prediction of VLE at 343 K and H^E at 298 K based on the optimised parameters from VLE measurements at 1 atm is presented in Figure 1.4.

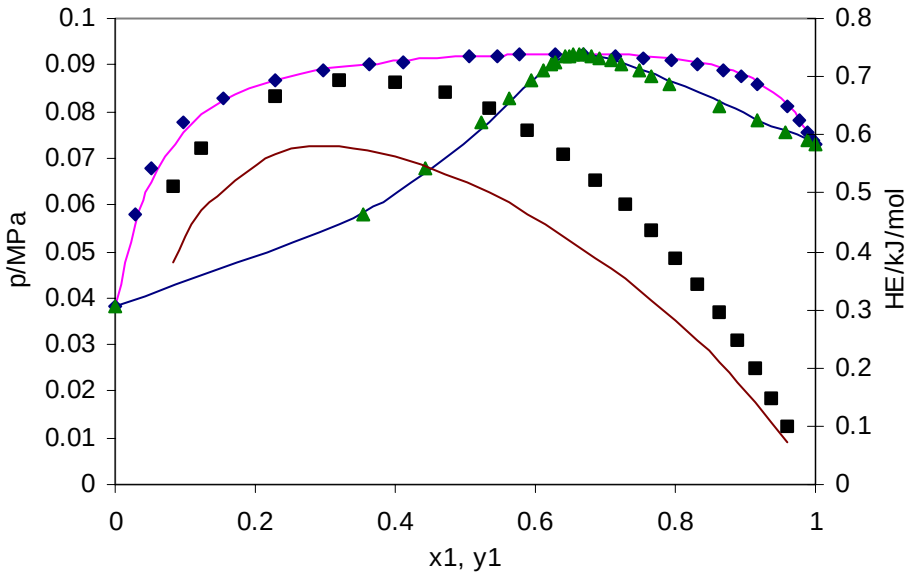

Figure 1.4 *Only VLE data at 1 atm used in optimisation of parameters. The parameters were used in the prediction of VLE at 343 K and* H^E *at 298 K.* ◆, x_1 *at 343 K;* ▲, y_1 *at 343 K;* ■, H^E *at 298 K;* —, *model.*

VLE is predicted well but the AARE in H^E is 24.4 %. The prediction of VLE at 1 atm and H^E at 298 K based on the optimised parameters from VLE measurements at 343 K is presented in Figure 1.5.

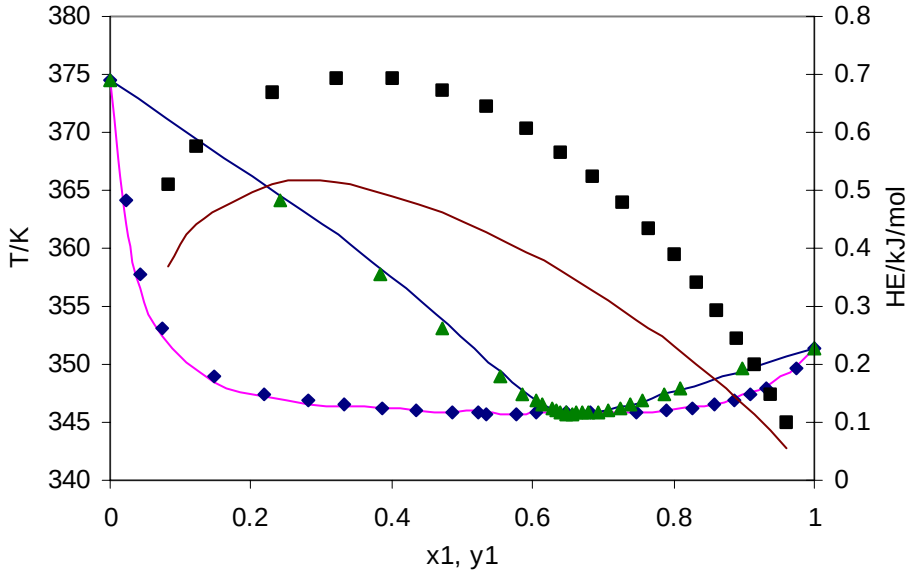

Figure 1.5 *Only VLE data at 343 K used in optimisation of parameters. The parameters were used in the prediction of VLE at 1 atm and H^E at 298 K.* ◆, *x_1 at 1 atm;* ▲, *y_1 at 1 atm;* ■, *H^E at 298 K*; —, *model.*

The VLE is predicted well but the AARE in H^E is 35.6 %. The prediction of VLE at 1 atm and VLE at 343 K based on the optimised parameters from H^E measurements at 298 K is presented in Figure 1.6.

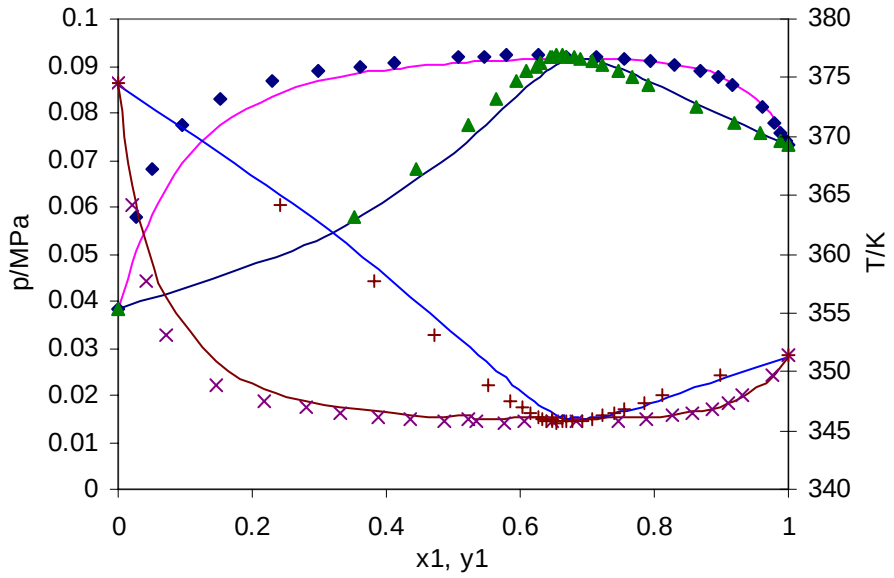

Figure 1.6 *Only H^E data at 298 K used in optimisation of parameters. The parameters were used in the prediction of VLE at 1 atm and VLE at 343 K.* ◆, *x_1 at 343 K;* ▲, *y_1 at 343 K;* ×, *x_1 at 1 atm;* +, *y_1 at 1 atm;* —, *model.*

In this case AARE in temperature of isobaric measurement is 0.18 % and AARE in pressure of isothermal data is 2.43 %. In this case the parameters optimised based on the excess enthalpy measurements gave good prediction of VLE. The subject if excess enthalpy measurements only could be an alternative for VLE measurements has been discussed in literature. Nicolaides and Eckert (1978) and Skjold-Jørgensen et al. (1980) found that contradictory conclusions were made in the literature and the prediction of VLE data based on the parameters of excess enthalpy measurements was usually unsuccessful.

One option to increase the accuracy of the modelling is to increase the number of parameters, from 2 to 4 and from 4 to 6, as presented in Table 1.3.

Table 1.3 *Approximate confidence limits and approximate correlation coefficient matrix for system ethanol + 2,4,4-trimethyl-1-pentene with 4 or 6 Wilson parameters.*

VLE at 1 atm and 343 K and HE at 298 K

a_{ij}	conf. limit	low limit a_{ij}	high limit a_{ij}	The appr. correlation coefficient matrix.			
10746.8	1166.0	9580.8	11912.8	1	-0.707	-0.996	0.174
1807.3	65.9	1741.4	1873.3	-0.707	1	0.757	-0.657
-8.4	3.2	-11.5	-5.2	-0.996	0.757	1	-0.250
-2.9	0.3	-3.3	-2.6	0.174	-0.657	-0.250	1
AARE in T/%		0.04					
AARE in p/%		0.40					
AARE in HE/%		1.93					

VLE at 1 atm and 343 K and HE @ 298 K

a_{ij}	conf. limit	low limit a_{ij}	high limit a_{ij}	The appr. correlation coefficient matrix.					
10746.3	1245.7	9500.7	11992.0	1	-0.739	-0.996	0.216	0.357	-0.181
1808.0	72.8	1735.3	1880.8	-0.739	1	0.789	-0.662	-0.425	0.220
-8.4	3.5	-11.8	-4.9	-0.996	0.789	1	-0.291	-0.403	0.202
-2.9	0.4	-3.2	-2.5	0.216	-0.662	-0.291	1	0.182	-0.131
2.3E-05	4.4E-04	-4.2E-04	4.6E-04	0.357	-0.425	-0.403	0.182	1	-0.412
1.4E-06	3.2E-05	-3.1E-05	3.4E-05	-0.181	0.220	0.202	-0.131	-0.412	1
AARE in T/%		0.03							
AARE in p/%		0.40							
AARE in HE/%		1.94							

When the number of parameters was changed from 2 to 4 the accuracy increased but there was a minor increase in the accuracy when the number of parameters was changed from 4 to 6. When six parameters were used the last two parameters were close to zero and confidence level was bigger than the absolute value of the parameter meaning that four parameters were sufficient. The correlated VLE and H^E with the four-parameter model is presented in Figures 1.7 and 1.8

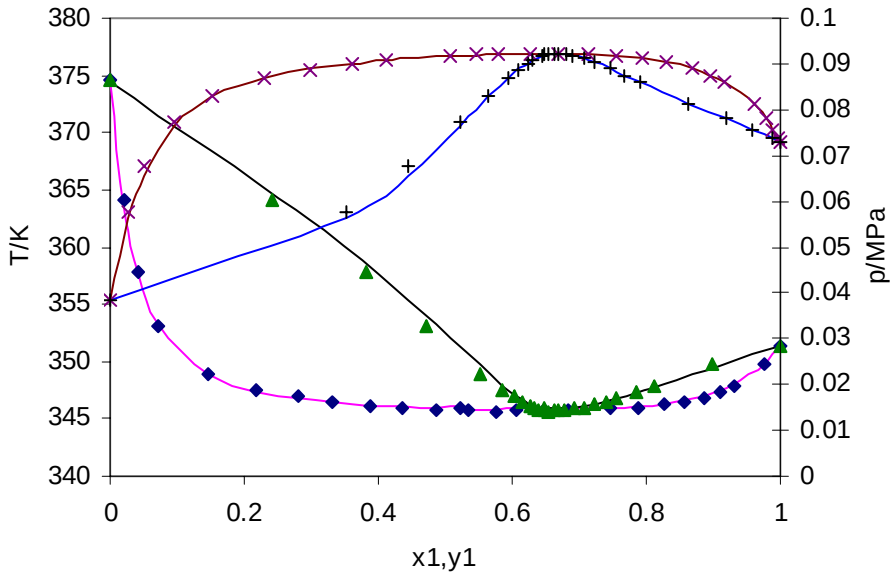

Figure 1.7 *Measured VLE data at 1 atm and 343 K and H^E at 298 K used in optimisation of 4 parameters of Wilson model, VLE reproduced.* ◆, x_1 at 1 atm; ▲, y_1 *at 1 atm;* ×, x_1 *at 343 K;* +, y_1 *at 343 K;* —, *model.*

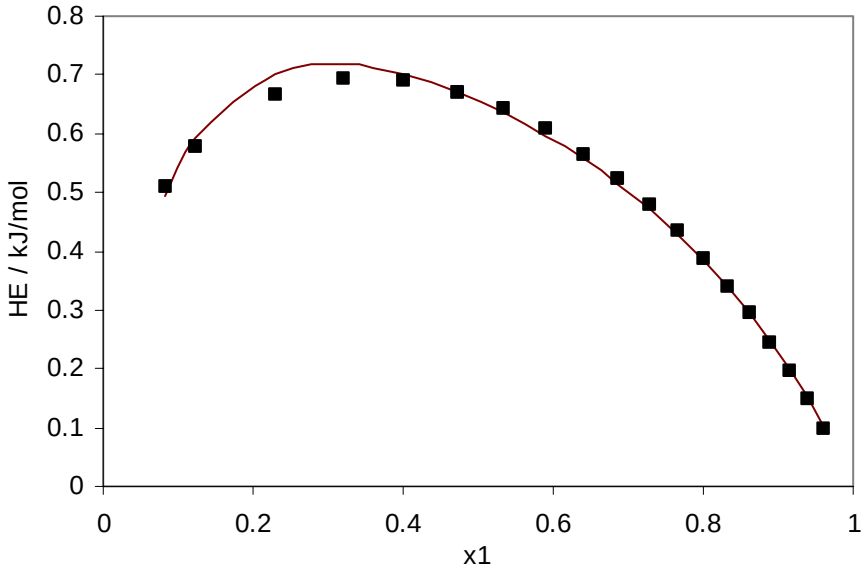

Figure 1.8 *Measured VLE data at 1 atm and 343 K and H^E at 298 K used in optimisation of 4 parameters of Wilson model, H^E reproduced.* ■, H^E *at 298 K*; —, *model.*

In this case the optimised values of two-parameter model were used as initial values of the four-parameter model, and the optimised values of the four-parameter model were used as initial values of six-parameter model. However, if optimised values of the two-parameter model and the initial values of the rest four parameters as zero were used a different set of optimised parameters were obtained.

2 Vapour liquid flash near the critical point

The motivation for the development of a vapour liquid flash at constant pressure and temperature (pT-flash) came from the dynamic simulation of pressure relief systems, discussed in papers [IX]-[X]. The vapour liquid pT-flash answers the question about the amount and the composition of the phases. The pT-flash is the "work horse" routine that is called several times during a simulation. If the pT-flash cannot give a reliable answer, the whole dynamic simulation fails.

Traditional design of relief systems assumes stationary relieving conditions. This approach does not provide the important dynamics of the system. Traditional design methods are also meant for conditions far from the thermodynamic critical point. The vicinity of the critical point and the transition of the relieving fluid between the single and the two phases are an extra challenge in the dynamic simulation. In this thesis, the flash and the dynamic simulation are limited to the vapour liquid equilibrium, not to liquid-liquid or multiphase equilibrium.

The techniques to solve flash problem is discussed for example by Ohanomah and Thompson (1984), Nelson (1987), Bünz et al. (1991) and Sofyan et al. (2003). There are two techniques to solve the flash problems: the fugacity-matching method or the Gibbs energy minimisation technique.

The flash is traditionally solved by equalising the fugacity of components in each phase. The number of phases is guessed and the vaporisation equilibrium ratios are estimated. Then balances are solved for mole fractions and vaporisation equilibrium ratios are updated either from the equations of state or the activity coefficient approach. Convergence is reached when changes in mole fractions and amounts of phases are below tolerance. The early paper of Rachford and Rice (1952) that uses this technique is probably the most cited paper. Nelson (1987) and Bünz et al. (1991) used this technique for multiphase cases and Ohanomah and Thompson (1984) reviewed the variations of this technique.

The Gibbs energy minimisation routines try to reach the global minimum of Gibbs free energy. The paper of Gautam and Seider (1979) seems to be the paper that started the intense research in Gibbs energy minimisation techniques. The Gibbs energy minimisation technique allowed the reaction to take place. According to Sofyan et al. (2003), the energy minimisation methods of Gibbs are superior to the fugacity matching methods, because the phase stability and phase split are solved simultaneously. Practically, the free energy minimisation technique produces analogous but more complex equations compared to fugacity matching. The problem in Gibbs energy minimisation is the location of the global minimum. Various alternatives to guarantee the global minimum have been developed. Amman and Renon (1987) combined traditional flash and Gibbs energy minimisation. Michelsen (1982a) formulated Gibbs energy problem as the tangent plane distance and multiple initial guesses. For the unstable phase, the tangent plane distance is negative. Sun and Seider (1995) used a homotopy-continuation method to guarantee the global minimum. The homotopy-continuation method provides a smooth transition between

the approximate solution and the true solution of a particular equation through the use of homotopy parameter. Nichita et al. (2002) used the global optimisation method, tunnelling, to find the global minimum. Sofyan et al. (2003) eliminated the initial guessing problem by generating a grid of initial guesses and this way reached the global minimum.

The research on flash is intense and numerous methods are proposed. All the methods seem to be developed for a particular problem, and guaranteed convergence to the correct solution for any problem is still the challenge.

2.1 The pT-flash

The flash at constant pressure and temperature is needed very frequently in determining the phase of the mixture of known total composition. If it is known beforehand that the mixture is in two phases, liquid and vapour, the formulation of the flash is much simpler than in the case where the mixture can also be in a single phase, liquid or vapour.

The supercritical mixture is not treated separately. It is liquid-like or vapour-like. This may be confusing, but the terminology for the supercritical mixture is not uniform enough. A one-component fluid is supercritical if the temperature and pressure are higher than the critical temperature and critical pressure. But a multi-component mixture can be a mixture of two phases when the temperature and pressure are higher than the critical temperature and critical pressure, see the examples presented later.

2.1.1 Generation of initial K_i-values

At a given temperature T and pressure p the initial values for the vaporisation equilibrium ratios K_i are generated from the Wilson (1968) approximation.

$$\ln(K_i) = \ln\left(\frac{p_{c,i}}{p}\right) + 5.373(1-\omega_i)\left(1-\frac{T_{c,i}}{T}\right) \tag{2.1}$$

Wilson approximation is a direct application of Raoult's law

$$K_i = \frac{p_i^{sat}}{p} \tag{2.2}$$

where vapour pressure is generated by forcing a Clausius-Clapeyron relationship through two points, the critical point and the point defined by the acentric factor, Trebble (1989). Derivation shows that at the critical point, the Clausius-Clapeyron equation, sometimes also called the two-parameter correlation of Antoine, is

$$\ln(p_{c,i}) = A_i - \frac{B_i}{T_{c.i}} \tag{2.3}$$

The definition of the acentric factor is

$$\log\left(p_{r,i}^{sat,T_r=0.7}\right) = -\omega_i - 1 \tag{2.4}$$

Changing the base of the logarithm

$$\frac{\ln\left(p_{r,i}^{sat,T_r=0.7}\right)}{\ln(10)} = -\omega_i - 1 \tag{2.5}$$

and converting the reduced vapour pressure to the vapour pressure

$$\ln\left(p_i^{sat,T_r=0.7}\right) = -\ln(10)(\omega_i + 1) + \ln\left(p_{c,i}\right) \tag{2.6}$$

At the reduced temperature $T_r = 0.7$ the Clausius Clapeyron relationship is

$$-\ln(10)(\omega_i + 1) + \ln\left(p_{c,i}\right) = A_i - \frac{B_i}{0.7 \cdot T_{c,i}} \tag{2.7}$$

Solving constant A_i from (2.3) we get

$$A_i = \ln\left(p_{c,i}\right) + \frac{B_i}{T_{c,i}} \tag{2.8}$$

and inserting to (2.7)

$$-\ln(10)(\omega_i + 1) + \ln\left(p_{c,i}\right) = \ln\left(p_{c,i}\right) + \frac{B_i}{T_c} - \frac{B_i}{0.7 \cdot T_{c,i}} \tag{2.9}$$

and solving B_i

$$B_i = \frac{-\ln(10)(\omega_i + 1)T_{c,i}}{\left(1 - \frac{1}{0.7}\right)} \tag{2.10}$$

Applying the Clausius-Clapeyron equation at T and p with solved A_i and B_i we get

$$\ln\left(p_i^{sat}\right) = \ln\left(p_{c,i}\right) + \frac{-\ln(10)(\omega_i + 1)T_{c,i}}{\left(1 - \frac{1}{0.7}\right)T_{c,i}} - \frac{-\ln(10)(\omega_i + 1)T_{c,i}}{\left(1 - \frac{1}{0.7}\right)T} \tag{2.11}$$

Taking the natural logarithm of K_i -value

$$\ln(K_i) = \ln\left(p_i^{sat}\right) - \ln(p) \tag{2.12}$$

we see that

$$\ln(K_i) = \ln\left(\frac{p_{c,i}}{p}\right) + \frac{\ln(10)(\omega_i + 1)}{\left(1 - \frac{1}{0.7}\right)}\left(1 - \frac{T_{c,i}}{T}\right) \approx \ln\left(\frac{p_{c,i}}{p}\right) + 5.373(\omega_i + 1)\left(1 - \frac{T_{c,i}}{T}\right) \tag{2.13}$$

This Wilson approximation is crucial in starting the flash. The approximation is simple in the sense that it only needs the critical temperature, critical pressure and the acentric factor of individual components.

2.1.2 Stability analysis to improve initial K_i-values

If the minimum of the K_i-values from the Wilson approximation is greater than 1.0 or the maximum of the K_i-values is less than 1.0, a stability analysis is performed. In this work, the stability analysis is used to improve the initial estimates of K_i-values. According to Michelsen (1982 a & b) a stability analysis is a procedure to get better initial estimates for K_i-values and to find out if the phase is stable or not. The stability analysis is divided into two parts. At first the feed $\boldsymbol{z}$ is assumed liquid and vapour-like trial phase $\boldsymbol{w}$ is generated with Wilson K_i-values.

$$w_i = K_i z_i \tag{2.14}$$

The equation of state is called to get the fugacity coefficients for the vapour trial phase and liquid feed phase. A modified tangent plane distance is computed

$$tm(\boldsymbol{w}) = 1 + \sum w_i \left(\ln(w_i) + \ln(\varphi_i(\boldsymbol{w})) - d_i - 1\right) \tag{2.15}$$

where

$$d_i = \ln(z_i) + \ln(\varphi_i(\boldsymbol{z})) \tag{2.16}$$

Now it is possible to iterate the new vapour trial phase composition with successive substitution

$$\ln\left(w_i^{k+1}\right) = d_i - \ln\left(\varphi_i\left(\boldsymbol{w}^k\right)\right) \tag{2.17}$$

The successive substitution loop is continued until converged. The fugacity coefficients of converged trial vapour phase and feed liquid phase give the updated K_i-values. If the minimum of the modified tangent plane distance of the liquid and vapour trial phase is positive, the feed phase is stable.

The successive substitution procedure is repeated for the vapour feed phase and liquid trial phase, where the liquid-like trial phase is generated obtaining K_i-values from the Wilson approximation.

$$w_i = \frac{z_i}{K_i} \tag{2.18}$$

If the minimum of the modified tangent plane distance of the vapour and liquid trial phase is positive, the feed phase is stable. There are also trivial solutions of the successive substitution loops that are indications of a stable feed phase, but these are found by a tedious trial and error procedure.

If the difference between maximum and minimum K_i-values generated with stability analysis is less than a defined tolerance, it indicates that the stability analysis has failed in producing better initial estimates. Then the Wilson approximation K_i-values are computed once again, because they are the best estimates at the moment. The K_i-values are updated based on the stability analysis only when the modified tangent plane distance is negative. For the vapour-like trial phase

$$\ln(K_i) = \ln(\varphi_i(\boldsymbol{z})) - \ln(\varphi_i(\boldsymbol{w})) \tag{2.19}$$

and for liquid-like trial phase

$$\ln(K_i) = \ln(\varphi_i(\boldsymbol{w})) - \ln(\varphi_i(\boldsymbol{z})) \tag{2.20}$$

It is empirically found in my work that the minimum of vapour-like and liquid-like modified tangent plane distances is selected.

$$tm_{\min} = \min(tm_{vt}, tm_{lt}) \tag{2.21}$$

If $tm_{\min}$ is greater than zero either liquid or vapour phase is stable.

Trivial solution is found if

$$\Delta K_{vt} = K_{i,\max,vt} - K_{i,\min,vt} \le \varepsilon \text{ and } \Delta K_{lt} = K_{i,\max,lt} - K_{i,\min,lt} \le \varepsilon \text{ and } tm_{\min} > 0 \tag{2.22}$$

Vapour K_i -values are set as initial K_i -values if

$$\Delta K_{vt} > \Delta K_{lt} \text{ and } \Delta K_{lt} > \varepsilon \text{ and } K_{i,\min,vt} < 1 \text{ and } K_{i,\max,vt} > 1 \tag{2.23}$$

Liquid K_i -values are set as initial K_i -values if

$$\Delta K_{lt} > \Delta K_{vt} \text{ and } \Delta K_{vt} > \varepsilon \text{ and } K_{i,\min,lt} < 1 \text{ and } K_{i,\max,lt} > 1 \qquad (2.24)$$

Vapour K_i -values are set as initial K_i -values also if

$$tm_{\min} < 0 \text{ and } tm_{vt} > tm_{lt} \text{ and } \Delta K_{lt} > \varepsilon \qquad (2.25)$$

Liquid K_i -values are set as initial K_i -values also if

$$tm_{\min} < 0 \text{ and } tm_{lt} > tm_{vt} \text{ and } \Delta K_{vt} > \varepsilon \qquad (2.26)$$

2.1.3 Newton iteration

The flash equations can be derived from the basic equations. The amount of liquid n_l and vapour n_v in moles at a specified temperature and pressure can be solved from the material balances of a system

$$n_f = n_l + n_v \qquad (2.27)$$

$$n_f z_i = n_l x_i + n_v y_i \qquad (2.28)$$

$$y_i = K_i x_i \qquad (2.29)$$

$$\beta = \frac{n_v}{n_f} \qquad (2.30)$$

where n_f is the molar feed, z_i, x_i and y_i are the mole fraction of component i in feed, liquid, and vapour, respectively. The vapour fraction β describes the ratio of moles of vapour to the moles of feed. The vaporisation equilibrium ratio K_i of component i measures the tendency to partition itself between liquid and vapour.

$$K_i = \frac{y_i}{x_i}$$

Solving for y_i and x_i and we get

$$y_i = \frac{K_i z_i}{1 - \beta + \beta K_i} \qquad x_i = \frac{z_i}{1 - \beta + \beta K_i} \qquad (2.31 \text{ a \& b})$$

Inserting the equations (2.31 a & b) to the objective function (2.32) that usually guarantees the best convergence

$$g(\beta) = \sum_{i=1}^{C} (y_i - x_i) = 0 \qquad (2.32)$$

gives the Rachford-Rice (1952) equation

$$g(\beta) = \sum_{i=1}^{C} z_i \frac{K_i - 1}{1 - \beta + \beta K_i} = 0 \qquad (2.33)$$

The Rachford-Rice equation is not the only way to formulate the function for the Newton iteration. Ohanomah and Thompson (1984) have listed alternatives for the Rachford-Rice equation.

Rachford-Rice equation is called at vapour fraction 0.0, 0.5, and 1.0 to get the function values. If the function changes its sign in the range from 0 to 0.5, the initial

value $\beta = 0.25$ and if it changes its sign in the range from 0.5 to 1, the initial value $\beta = 0.75$ is suitable.

The smallest K_{min} and the greatest K_{max} are searched to solve the greatest and smallest value of vapour fraction, respectively.

According to Whitson and Michelsen (1989), the asymptotes occur at values $\beta = 1/(1-K_i)$. There is a solution between all asymptotes, but the only solution to produce non-negative compositions y_i and x_i is between

$$\beta_{min} = \frac{1}{1-K_{max}} \qquad \beta_{max} = \frac{1}{1-K_{min}} \tag{2.34 a \& b}$$

According to Whitson and Michelsen (1989) the physical limits $\beta = 0$ and $\beta = 1$ are inside the minimum and maximum vapour fraction

$$\beta_{min} < 0 < 1 < \beta_{max} \tag{2.35}$$

when

$$K_{min} < 1 \qquad \text{and} \qquad K_{max} > 1 \tag{2.36}$$

Vaporisation equilibrium ratios are tested again. If the smallest K_{min} is greater than the unity or the greatest K_{max} is smaller than the unity, the single phase is stable because the stability analysis is already called before. Return to calling subroutine.

The Rachford-Rice (1952) is solved with the Newton method that needs the derivative of g with respect to vapour fraction β.

$$g(\beta)' = -\sum_{i=1}^{C} z_i \frac{(K_i - 1)^2}{(1 - \beta + \beta K_i)^2} \tag{2.37}$$

According to Mollerup and Michelsen (1996), there are two cases when the convergence is very slow. When a very volatile component is present in small amount in feed and the solution is close to $\beta = 0$ or very heavy component is present in small amount and the solution is close to $\beta = 1$. In these cases, the derivative of g is big, and thus the convergence is very slow.

The round-off errors may corrupt the result if vapour fraction β is close to 1 and very heavy components are present. Digits are lost in the subtraction of $1-\beta$ in the denominator $(1 - \beta + \beta K)$. Mollerup and Michelsen (1996) suggested using

$$g(\beta_l) = \sum_{i=1}^{C} z_i \frac{K_i - 1}{\beta_l + (1 - \beta_l) K_i} = 0 \tag{2.38}$$

and

$$g(\beta_l)' = -\sum_{i=1}^{C} z_i \frac{(K_i - 1)^2}{(\beta_l + (1 - \beta_l) K_i)^2} \tag{2.39}$$

where $\beta_l = 1 - \beta$.

Function g is monotonically decreasing and the solution is at the interval 0...1 if

$$g(0) = \left(\sum_{i=1}^{C} z_i K_i \right) - 1 > 0 \tag{2.40}$$

and

$$g(1) = 1 - \sum_{i=1}^{C} \frac{z_i}{K_i} < 0 \qquad (2.41)$$

When $g(0) < 0$ the phase is a subcooled liquid and when $g(1) > 0$ the phase is a superheated vapour.

The Newton step size is limited between the minimum and maximum vapour fraction. If the step size would hit outside the range of the vapour fraction, the new step is the average of the present and the boundary value for the vapour fraction. The iteration is continued if stopping criteria is bigger than the tolerance and the number of iterations is less than 1000.

2.1.4 Successive substitution

After the inner Newton iteration loop the K_i-values are updated from an equation of state.

$$\ln K_i = \ln \frac{y_i}{x_i} = \ln \frac{\phi_i^l(T, p, \boldsymbol{x})}{\phi_i^v(T, p, \boldsymbol{y})} \qquad (2.42)$$

The liquid and vapour composition needed in the equation of state is computed from the Rachford-Rice equation with solved vapour fraction. The successive substitution loop goes back to the Newton iteration to solve vapour fraction. Successive substitution is continued if the absolute difference between the previous and updated K_i-values is bigger than the tolerance and the number of iterations is less than 1000. The flash is converged when both the Newton iteration and the successive substitution loop is converged.

2.1.5 Methods to recover the fail of flash

If the number of successive substitution loops exceeds the maximum, it is an indication that the temperature and pressure are very close to the critical point or outside the convergence pressure envelope. Whitson and Michelsen (1989) presented the concept of convergence pressure envelope. It is the mathematical phase boundary where the mole fractions are still positive but the vapour fraction is outside the physical limits. The critical point causes a lot of trouble also in this routine. It seems to be known but not accepted by the users that the flash does not converge near the critical point. I have developed additional routines to handle the vicinity of the critical point. If the flash fails, complex and central processing unit (CPU) time consuming routines are started to recover from the very unfortunate failing.

2.1.5.1 Initial point generation

At first the critical point is computed with the method of Heidemann and Khalil (1980), see also [VIII] where the equations of state used in this work are explained.

Next the phase envelope is computed. It needs a good initial point but the guessing of the initial point must be done automatically, because there is no easy way to allow any

user action. The approach developed in this work was to use the equation of state that was already used in the flash routine and not to use the vapour pressure correlations that we have not required this far. The total composition is known in pT-flash and we do not need to guess the vapour or liquid compositions. The initial guess is generated with the property of a cubic equation of state that there is a region of three roots at the specified total composition.

Several researchers have studied the number of roots of the cubic equation of state. The motivation for studies has mainly been failing of flash, trivial solution, efficiency of solution, and the usage of complex roots to achieve correct root. As far as I know the previous studies have not studied the initial point generation. Coward et al. (1978) and Poling et al. (2001) among many others studied the solution of cubic equation of state and where it has one or three roots. Gundersen (1982) studied the failures in flash calculation and solving the wrong type of root. He warned about the connection between number of roots arising from cubic equation of state and the actual number of phases. Gosset et al. (1986) studied the efficiency of solution algorithms for cubic equations of state and discussed the number of roots. Lucia and Taylor (1992) studied the complex roots of cubic equations of state.

The generation of a good initial point starts at defined low pressure, for example 0.1 MPa abs. The pressure is selected empirically and the total composition is known in the pT-flash. The number of roots of the cubic equation of state is calculated from the lower to upper temperature. The empirically selected lower temperature is 50 K and the upper temperature is 1000 K. This temperature range covers a great number of components used in the hydrocarbon processing industry, except hydrogen. It is found that at 50 K the cubic equation of state should give one root for almost all components. The temperature is increased with 2.5 K steps and the calculation of the number of roots is repeated. Sooner or later the number of roots changes from one to three and this temperature is stored. As the temperature increases, the number of roots changes soon from three to one again and the temperature is stored. The generated initial temperature is simply the average of these two stored temperatures. The initial temperature usually hits between the dew and bubble point curve and makes it possible to start either the dew or bubble point calculation. This initial point generation very seldom fails and it provides a good initial point for bubble or dew point temperature.

For pure components, the vapour pressure correlation, like Antoine, could be used for the initial temperature calculation at a specified pressure. In fact, it would give the initial pressure with high accuracy when the saturated temperature at a specified pressure is solved. However, the method developed in this work performs well for both the pure component and the mixtures.

It should be remembered that if three roots are found it does not indicate that two phases are in equilibrium. This property has very little to do with rigorous thermodynamics, but in my opinion it is the easiest way to generate a good initial point. The number of roots is conveniently found by analytical solution of a third order equation.

2.1.5.2 Construction of phase envelope

As the initial point is generated, the saturation temperature at specified pressure must be calculated. The phase envelope can be started either from the bubble point or dew point side but in practice there are exceptions. Usually the bubble point side of the phase envelope of hydrogen containing mixture curves upward at a low temperature but the dew point side behaves normally. This is the most important reason that the construction of a phase envelope is started from the dew point side in the flash routines.

One method to construct the phase envelope is the series of bubble and dew point calculations presented by Ziervogel and Poling (1983). They controlled the variable to be solved by dimensionless slope of the phase envelope

$$\beta_{ZP} = \left| \frac{d(\ln p)}{d(\ln T)} \right| \qquad (2.43)$$

When $\beta_{ZP} < 2$ they solved dew or bubble point pressure and when $\beta_{ZP} > 20$, they solved dew or bubble point temperature. Values of $2 < \beta_{ZP} < 20$, either pressure or temperature can be solved.

Another set of methods to compute the phase envelope is presented in the papers of Michelsen (1980) and Michelsen (1994). The Michelsen (1994) method is selected for the recovering routines of pT-flash because I found it easier to start than the earlier method. The phase envelope starts at the solved bubble or dew point temperature, continues towards the critical point, passes it, and ends to the opposite side than from where it started. The following is a short presentation of the method.

The Michelsen (1994) method differs from the Michelsen (1980) method of constructing the phase envelope. In the Michelsen (1994) method there are three variables, which are temperature, pressure, and variable α that acts as a specified variable that drives the set of solutions through the phase envelope. In the Michelsen (1980) method, the number of variables is the number of components plus two variables, namely ln(K_i)-values, temperature and pressure.

According to Michelsen (1994) if $\boldsymbol{y}$ is considered always as an incipient phase and $\boldsymbol{z}$ as the overall composition, at equilibrium the following equations apply

$$\ln y_i + \ln\phi_i(\boldsymbol{y}) - \ln z_i - \ln\phi_i(\boldsymbol{z}) = 0 \qquad (2.44)$$

$$\sum_i^C (y_i - 1) = 0 \qquad (2.45)$$

The construction of a phase envelope starts by solving a bubble or dew point at low pressure. The reference K_i-values are computed based on the solved bubble or dew point. Equation (2.46 a) is valid for bubble point and (2.46 b) for dew point

$$\ln K_i^* = \ln \frac{y_i^*}{z_i} \quad \ln K_i^* = \ln \frac{z_i}{y_i^*} \qquad (2.46\ \text{a \& b})$$

where the y_i^* is the mole fraction of the component i in the incipient phase, it is vapour at the bubble point side and liquid at the dew point side of the phase envelope. The total composition z_i is liquid at the bubble point side and vapour at the dew point side of the phase envelope. Equations (2.44) and (2.45) can be replaced with the following equations

$$f_1(T, p, \alpha) = \sum_{i=1}^{C} y_i d_i = 0 \tag{2.47}$$

$$f_2(T, p, \alpha) = \sum_{i=1}^{C} z_i d_i = 0 \tag{2.48}$$

The function f_1 is according to Michelsen (1994) the tangent plane distance for the mixture evaluated at composition $\boldsymbol{y}$. The function f_2 is needed to ensure the continuity of the phase envelope at the critical point. The third equation needed in providing the same number of equations and variables is

$$f_3 = \alpha - S = 0 \tag{2.49}$$

These equations can be solved with the full Newton method. In the beginning of the calculation the specified variable α is equal to one if computation is started from the bubble point side and minus one if started from the dew point side. Variable α passes the value of zero and changes its sign. The composition of the incipient phase $\boldsymbol{y}$ is scaled according to equations (2.50) and (2.51)

$$\ln Y_j = \ln z_j + \alpha \ln K_j^* \tag{2.50}$$

$$y_i = \frac{Y_i}{\sum_j Y_j} \tag{2.51}$$

The elements d_i in functions f_1 and f_2 are found from

$$d_i = \ln y_i + \ln \phi_i(\boldsymbol{y}) - \ln z_i - \ln \phi_i(\boldsymbol{z}) \tag{2.52}$$

The fugacity coefficients of phases are calculated with rigorous thermodynamics. As the specified variable α is greater than zero, the vapour fugacity coefficients with composition $\boldsymbol{y}$ and liquid fugacity coefficients with composition $\boldsymbol{z}$ are required. As the specified variable α is less than zero, the liquid fugacity coefficients with composition $\boldsymbol{y}$ and vapour fugacity coefficients with composition $\boldsymbol{z}$ are required.

According to Michelsen (1994) there are two methods to refine the points of the approximate phase envelope. The simpler one is chosen because it does not require additional iterations and thus it is robust. The overall deviation of the method is calculated from

$$D_{dev} = \sum_{i=1}^{C} z_i d_i^2 \tag{2.53}$$

If the deviation D_{dev} becomes large then the new reference K_i-values are updated from

$$\ln K_i^* = \frac{1}{\alpha}\left[\ln \phi_i(\boldsymbol{z}) - \ln \phi_i(\boldsymbol{y})\right] \tag{2.54}$$

This method also needs a similar scaling factor $A_{scaling}$ and approximation of critical points as the method of Michelsen (1980) needs.

The next value of the specified variable α must be determined. This is very important, because α_{next} is the driving force which gets the construction of the phase envelope to proceed

$$\alpha_{next} = \alpha + A_{scaling}(\alpha - \alpha_{old}) \tag{2.55}$$

Scaling factor $A_{scaling}$ is needed in acceleration and in deceleration of the phase boundary construction. The number of iterations bigger than the predetermined number of iterations is an indication of the poor initial estimates of the variables and thus there is a risk that the iteration could fail. Then the next step of the specified variable should be smaller to ensure convergence. If the number of iterations is

smaller than the predetermined number of iterations, the next step can be longer because the previous estimation for the variables was good. The values for the scaling factor and the predetermined number of iterations is a compromise between the number of calculated points at the phase boundary and the speed of calculation.

If the steps in temperature and pressure in the vicinity of the critical point are long, then the actual value of the critical point can be approximated either using polynomial approximations (Michelsen (1980)) or more simply by linear approximations. The two points in both sides of the critical temperature and pressure are known and the slope is

$$\frac{dX_k}{d\alpha} = \frac{X_k - X_{k,old}}{\alpha - \alpha_{old}} \tag{2.56}$$

The value of the specified variable $\alpha = 0$ at the critical point, so the temperature and pressure in the critical point can be obtained linearly as a function of specified variable. The variables $X_{k,old}$ and $X_{k,crit}$ are old and the critical point value of the critical property, in this case $k = 1$ is critical temperature and $k = 2$ critical pressure.

$$X_{k,crit} = X_{k,old} + \frac{dX}{d\alpha}\left(0 - \alpha_{old}\right) \tag{2.57}$$

The benefit of the Michelsen (1994) method for phase envelope construction is its speed in multi-component mixtures because the number of variables in the method remains at three when the number of components increases. Furthermore, the composition derivatives of fugacity coefficients are avoided. The Michelsen (1994) method for the phase envelope is identical to the Michelsen (1980) method for binary mixtures and in multi-component mixtures there are only minor differences.

2.1.5.3 Cubic spline interpolation

At first the passing of the critical point is checked. The construction of phase envelope may fail if the bubble and dew point curves are very close to each other. It leads to a very sharp curve of the envelope near the critical point. A mixture of propane and propene as a close boiling mixture and a mixture of carbon dioxide and ethane as an azeotropic mixture, Davalos et al (1976), are the "best" examples where the phase envelope routines fail.

At recovering routines of pT-flash the points of the phase envelope are stored in the matrix. The index of the nearest point at the phase envelope is searched.

$$l_{\min} = \sqrt{\left(\frac{T - T_{pe}}{T}\right)^2 + \left(\frac{p - p_{pe}}{p}\right)^2} \tag{2.58}$$

where T and p are points where the flash failed and T_{pe} and p_{pe} are points at the phase envelope.

The maximum temperature and maximum pressure of the phase envelope are searched from the matrix.

If the temperature and pressure where the flash failed are higher than the maximum temperature and maximum pressure of the phase envelope, the phase at the failed point of flash is a single phase.

The determination of the phase becomes much more complicated as either the temperature or pressure or both, where the flash failed, are lower than the maximum temperature and maximum pressure. Interpolation is needed because the temperature and pressure where the flash failed do not match the discrete temperature and pressure points at the phase envelope.

One way to avoid interpolation would be to recalculate either the bubble or the dew point. In my opinion, it is better to use the successfully computed phase envelope than start bubble or dew point calculations that are prone to fail in the immediate vicinity of the critical point.

Before the cubic spline is fitted, the temperature or pressure points at the phase boundary on the both side of failing temperature and pressure are searched. Once these are known, the spline is fitted. The spline gives the pressure at the failing temperature and temperature at the failing pressure.

According to Roche and Li (1987) parabolic blending coefficients are generated by

$$\boldsymbol{a} = -1/2\,\boldsymbol{p}_1 + 3/2\,\boldsymbol{p}_2 - 3/2\,\boldsymbol{p}_3 + 1/2\,\boldsymbol{p}_4 \qquad (2.59\text{ a})$$

$$\boldsymbol{b} = \boldsymbol{p}_1 - 5/2\,\boldsymbol{p}_2 + 2\,\boldsymbol{p}_3 - 1/2\,\boldsymbol{p}_4 \qquad (2.59\text{ b})$$

$$\boldsymbol{c} = -1/2\,\boldsymbol{p}_1 + 1/2\,\boldsymbol{p}_3 \qquad (2.59\text{ c})$$

$$\boldsymbol{d} = \boldsymbol{p}_2 \qquad (2.59\text{ d})$$

where each $\boldsymbol{p}_i$ is a vector, in this case $\boldsymbol{p}_i = [i \quad T \quad p \quad \alpha]^T$. Function value $\boldsymbol{C}(t)$ is obtained from

$$\boldsymbol{C}(t) = \boldsymbol{a}t^3 + \boldsymbol{b}t^2 + \boldsymbol{c}t + \boldsymbol{d} \qquad (2.60)$$

where the parameter *t* varies from 0 to 1.

Interpolation of pressure at specified temperature requires that the parameter *t* satisfies $\boldsymbol{C}_2(t) - T_{spec} = 0$. This is most conveniently done by single variable Newton iteration. When the parameter t is solved the pressure is computed using the above coefficients.

Interpolation of temperature at a specified pressure requires that the parameter *t* satisfies $\boldsymbol{C}_3(t) - p_{spec} = 0$. When the parameter t is solved, the temperature is computed using the above coefficients.

2.1.5.4 Concluding the stable phase based on the phase envelope

There are many combinations and they are best shown by if-then-structure. If the critical point is passed then minimum distance from T & p to phase envelope, maximum temperature T_{max} at phase envelope and the maximum pressure p_{max} at phase envelope should be found by scanning the computed points.

if ($T < T_{max}$) then
    if($T > T_i$ and $T < T_{i+1}$ and $j < 2$) then
        calculate p_1 @ T with spline (2.61)
    end if
    if($T < T_i$ and $T > T_{i+1}$ and $j < 2$) then
        calculate p_2 @ T with spline (2.62)
    end if
    if($T > T_i$ and $T < T_{i+1}$ and $j = 2$) then
        calculate p_3 @ T with spline, see example 2.2.4 (2.63)
    end if
end if
if ($p < p_{max}$) then
    if($p > p_i$ and $p < p_{i+1}$ and $j < 2$) then
        calculate T_1 @ p with spline (2.64)
    end if
    if($p < p_i$ and $p > p_{i+1}$ and $j < 2$) then
        calculate T_2 @ p with spline (2.65)
    end if
    if($p > p_i$ and $p < p_{i+1}$ and $j = 2$) then
        calculate T_3 @ p with spline, see example 2.2.3 (2.66)
    end if
end if

if($T > T_{max}$ or $p > p_{max}$)
    stable, supercritical (2.67)
end if
if($T < T_{max}$ and $p > \max(p_1; p_2)$) then
    stable, outside two-phase region (2.68)
end if
if($T > \max(T_1; T_2)$ and $p < p_{max}$) then
    stable, outside two-phase region, see example 2.2.1 (2.69)
end if
if($T < T_{max}$ and $p < \min(p_1; p_2)$ then
    stable, gas phase (2.70)
end if
if($T < \min(T_1; T_2)$ and $p < p_{max}$) then
    stable, liquid phase (2.71)
end if

The drawback of this method is connected to the construction of phase envelope. If the generation of initial point or the passing of the critical point is unsuccessful this method does not work. This flash routine is also used in this thesis in the section of

density modelling. The set of 3105 points were flashed using original SRK as the thermodynamic model and 7 of them had a combination where the fitting of spline was not possible. For the methane (10 mol-%) + *n*-decane (90 mol-%), T = 444.261 K and p > 31.02 MPa the construction of phase envelope started at T_1 = 444.132 K, T_2 = 446.366 K, T_3 = 448.841 K, T_4 = 451.587 K, etc. at 0.1 MPa. Now the T hit between the first and the second point, not the second and the third point. The spline requires two points on the both sides. Of course the lower pressure for initialisation easily solves this problem.

2.2 Examples of pT-flash

2.2.1 Binary ethane + *n*-heptane

One test case studied by Monroy-Loperena (2001) is the binary system of ethane + *n*-heptane. The flash I developed in this work passed the test case well. The phase envelope is presented in Figure 2.1. It was found by the recovery routines of the flash that the flash (T = 490 K and p = 6.5 MPa) of the binary mixture near the computed critical point (T_c = 491.26 K and p_c = 6.391 MPa) where T_r = 0.997 and p_r = 0.983 was not at the region of two phases. According to Monroy-Loperena (2001) it should be in the region of two phases. However, Monroy-Loperena (2001) has not reported the values of critical properties or binary interaction parameters of Soave (1972) equation of state. The difference in the thermodynamic model is the reason for the discrepancy.

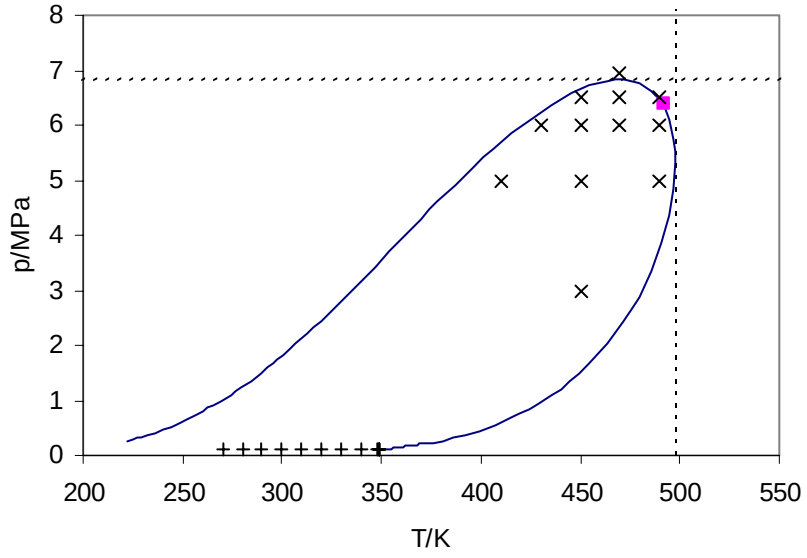

Figure 2.1. *Phase envelope of ethane + n-heptane.* ■*, critical point;* ×*, flashed point;* +*, initialisation of phase boundary;* - - - *, maximum temperature and pressure*

The initial K_i-values at T = 490 K and p = 6.5 MPa from the Wilson approximation gave K_1 = 6.9443 and K_2 = 0.2003. The bounds of the vapour fraction were 0.4159 < β < 0.6252. The initial value was set to β = 0.75 and the inner loop of the one variable Newton converged to β = 0.5411. The liquid and vapour mole fractions were calculated at the successive substitution loop to update K_i-values from equation of state giving K_1 = 2.1303 and K_2 = 0.447.

During the next iteration of the vapour fraction the bounds were 0.0576 < β < 0.9051, iteration converged to β = 0.4628, the update of K_i-values gave K_1 = 1.7065 and K_2 = 0.5625. This procedure continued but the successive loop did not converge. The Figure 2.2 presents the beginning of the iteration. When 1000 iterations were taken the value of vapour fraction was β = –94.4 and K_1 ja K_2 very close to unity.

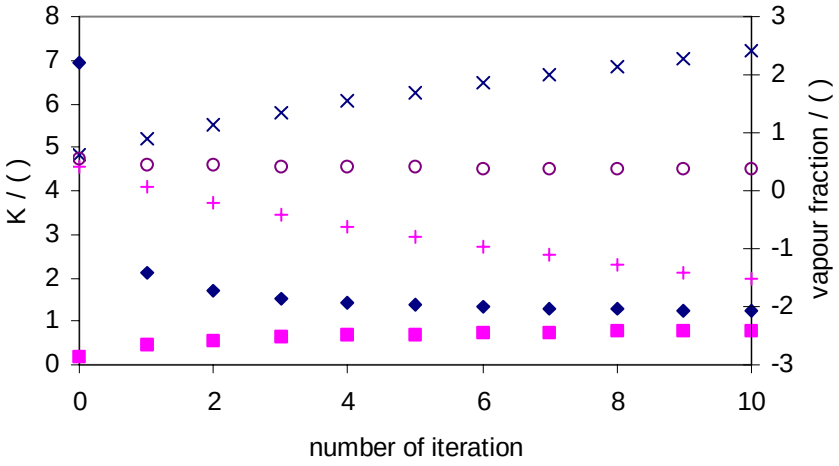

Figure 2.2 *Beginning of the iteration at T = 490 K and p = 6.5 MPa, ethane + n-heptane.* ◆, K_{max}; ■, K_{min}; +, β_{min}; ×, β_{max} ; ○, β.

There was no benefit to continue the iteration thus the single phase was concluded from the phase envelope. The three root region started at T = 135 K and ended at T = 405 K at 0.1 MPa, average of these was T = 270 K and it served as a starting point for the dew point temperature. The iteration of temperature from the stating point T = 270 K to dew point temperature is presented in Figure 2.1. The step length of Newton iteration was important in this case to prevent temperature to jump into the single phase (gas) region. The converged dew point temperature at 0.1 MPa was the starting point of phase envelope construction developed by Michelsen (1994). The points at phase envelope were stored in matrix for further tests.

Maximum temperature at phase boundary was T_{max} = 497.891 at 27th point and maximum pressure at phase boundary was p_{max} = 6827040 Pa at 33rd point. Because the flash temperature 490 K was lower than the T_{max} at phase boundary the point for the spline was constructed. The coefficients of the spline are presented in Table 2.1.

Table 2.1 *Points at phase boundary for splines, ethane + n-heptane*

	matrix of points for spline			
ith point	22	23	24	25
T/K	479.32	485.727	490.911	494.734
p/Pa	2874480	3353580	3852720	4357620
intern. var	-0.364804	-0.318855	-0.272905	-0.226955
	coefficients of spline			
ith point	0	0	1	23
T/K	-0.069965	-0.54099	5.79537	485.727
p/Pa	-7134.58	17152.4	489121	3353580
intern. var	0	5.55E-17	0.04595	-0.318855

The value of the spline parameter at T = 490 K was t = 0.803973. The spline gave the pressure p = 3754199 Pa.

The other set of points at the phase boundary enclosed the T = 490 K, it is presented in Table 2.2.

Table 2.2 *Points at phase boundary for splines, ethane + n-heptane*

	matrix of points for spline			
ith point	29	30	31	32
T/K	494.8	490.982	485.778	479.335
p/Pa	6110300	6407710	6628200	6767960
intern. var	-0.043156	0.002794	0.048743	0.094693
	coefficients of spline			
ith point	0	0	1	30
T/K	0.072995	-0.766021	-4.51077	490.982
p/Pa	-1920.75	-36531.3	258952	6407710
intern. var	0	0	0.04595	0.002794

The value of the spline parameter at T = 490 K was t = 0.21037. The spline gave the pressure p = 6460547 Pa at the phase boundary at T = 490 K.

Because the flash pressure 6500000 Pa is lower than the p_{max} at the phase boundary the same kind of procedure is repeated for pressure to get the temperatures. These two splines gave the temperatures T = 489.177 K and T = 441.288 K at the phase boundary at p = 6.5 MPa.

Finally, based on the temperatures and pressures from the spline the stability was tested. The flash temperature was higher than the spline temperature and the flash pressure was higher than the spline pressure, so the single phase was stable. This case the equation (2.69) was valid.

Another interesting point was T = 470 K and p = 6.95 MPa. It is found stable with the negative flash routine. The convergence of the negative flash is presented in Figure 2.3.

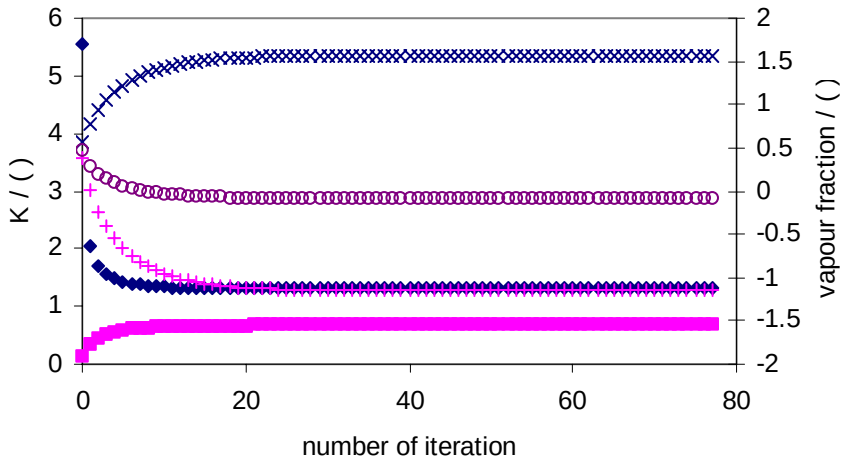

Figure 2.3 *Convergence of the iteration at T = 470 K and p = 6.95 MPa, ethane + n-heptane.* ◆, K_{max}; ■, K_{min}; +, β_{min}; ×, β_{max} ; ○, β.

Because the iteration converged to $\beta =$ -0.0823 the phase was the liquid phase. In this case no spline interpolation was needed. Whitson and Michelsen (1989) explained the convergence with the convergence phase envelope. It is the mathematical phase boundary where the mole fractions are still positive but the vapour fraction is outside the physical limits. The convergence pressure phase envelope was calculated with the method of Michelsen (1980) where the vapour faction was allowed to be beyond the physical limits. The convergence pressure phase envelope is presented in Figure 2.4.

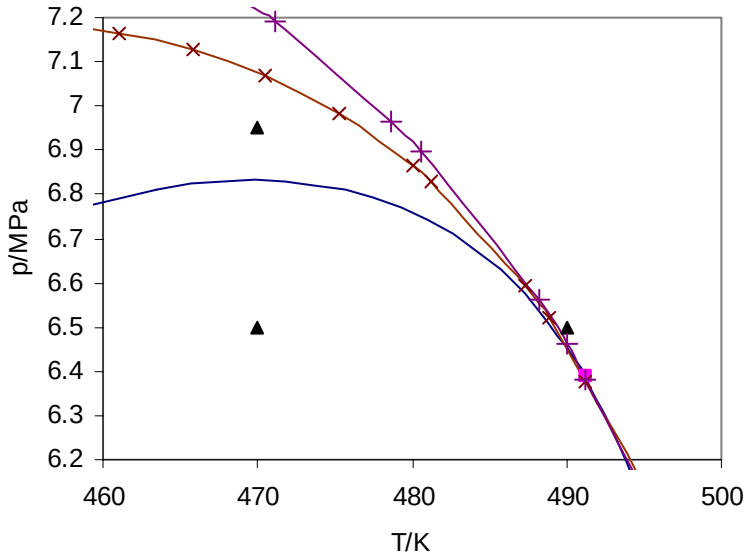

Figure 2.4 *Vicinity of the critical point of ethane + n-heptane.* —, *phase envelope;* ■, *critical point; solid line with* ×, *convergence pressure envelope at* β *= -0.2; solid line with* +, *convergence pressure envelope at* β *= -0.4;*

It can be seen that T = 490 K and p = 6.5 MPa is outside and T = 470 K and p = 6.95 MPa is inside the convergence envelope.

2.2.2 Mixture of 6 hydrocarbon components

Nichita et al. (2002) studied the synthetic mixture of 6 *n*-alkane, referred as the Y8 mixture in literature, mole fractions CH_4 = 0.8097, C_2H_6 = 0.0566, C_3H_8 = 0.0306, C_5H_{12} = 0.0457, C_7H_{16} = 0.033, $C_{10}H_{22}$ = 0.0244) components using PR, Peng and Robinson (1976), equation of state with all binary interaction parameters zero. This is an example of the mixture where there is a large region of two phases above the critical temperature and critical pressure. The phase envelope together with the convergence pressure envelope at β = 1.1 and β = -0.15 are presented in Figure 2.5

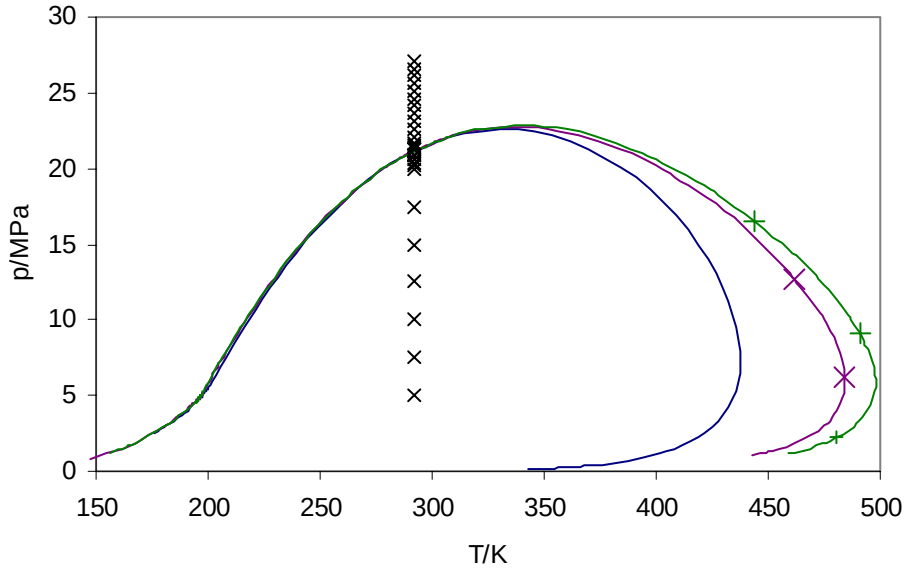

Figure 2.5 *Phase envelope of six component mixture. —, phase envelope; △, critical point; ×, flashed point; line with ×, convergence pressure envelope at β = 1.1; line with +, convergence pressure envelope at β = -0.15;*

At the region of two phases p_r = 0.990 was reached but at higher pressure the flash failed because the number of maximum iterations was reached. The vapour fraction, the limits of vapour fraction and the number of successive substitution loops to converge are presented in Figure 2.6. At reduced pressure p_r > 1 only number of successive substitution loops that converged to the trivial solution is shown.

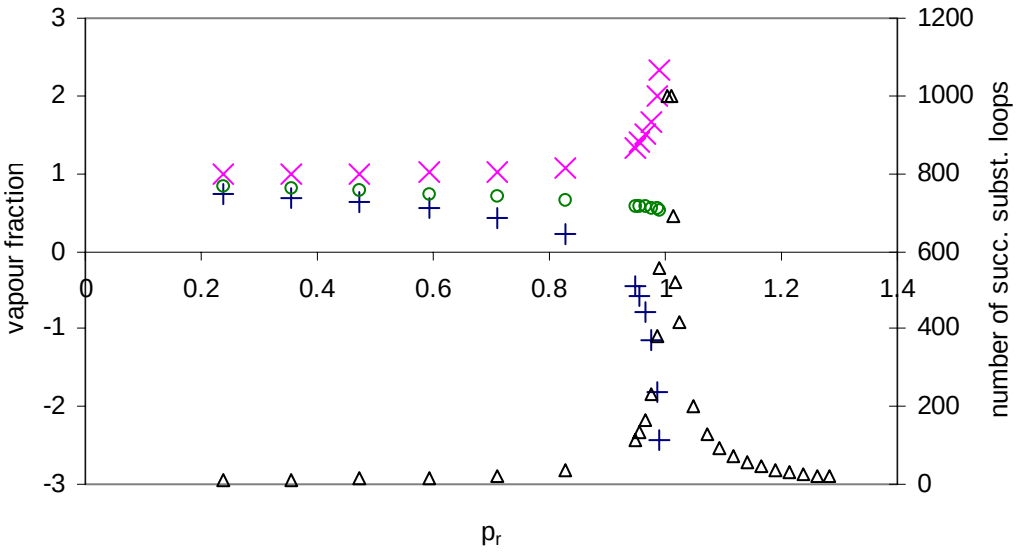

Figure 2.6 *Convergence of the iteration at the critical isotherm of the six component mixture.* +, β_{min}; ×, β_{max} ; ○, β; △, *number of successive substitution loops.*

In supercritical area the negative flash did not converge at $p_r = 1.009$ and $p_r = 1.014$ but the recovery routines found the single phase stable. At the higher pressures of the critical isotherm the iteration converged to trivial solution and found stable based on Rachford-Rice equation. The pressure convergence envelopes pass through the critical point. That's why it is difficult to get the negative flash to converge above the critical pressure and it requires the recovery routines developed in this work.

2.2.3 Ternary hydrogen + hydrocarbon mixture

One example is generated from the measurements of hydrogen + methane + propane reported in Knapp et al. (1989). SRK-DG, Graboski and Daubert (1979), SRK, Soave (1972) and PR, Peng-Robinson (1976), equations of state were used to calculate the bubble point pressure. The temperature dependence of the attraction term of SRK-DG is modified so that the binary interaction parameter between hydrogen and the other component is not needed. This modification requires also the special critical parameters for the hydrogen, $T_{c,H2} = 41.67$ K, $p_{c,H2} = 21.03$ bar = 20.75 atm, $\omega_{H2} = 0.0$. They differ from the measured ones. The binary interaction parameters of SRK and PR were set to zero. The binary interaction parameters were optimised for SRK and PR. The percent absolute relative error for the bubble point pressure and for the vapour mole fractions are presented below in Table 2.3. The SRK-DG is even better than SRK and PR with the optimised parameters in this case.

Table 2.3 *Average absolute percent error in pressure and vapour mole fraction*

	average absolute % error in			
	p	y, hydrogen	y, methane	y, propane
SRK-DG	9.1	6.2	30.8	37.9
SRK	12.1	12.1	38.0	39.0
PR	18.2	15.3	48.7	40.8
opt SRK	9.9	15.0	50.9	37.5
opt PR	9.6	14.7	52.0	37.2

From the recovery routines point of view the start of phase envelope construction is on the dew point side, start from the bubble point side is much more complicated. The recovery routines were not needed in the following points, see Figure 2.7

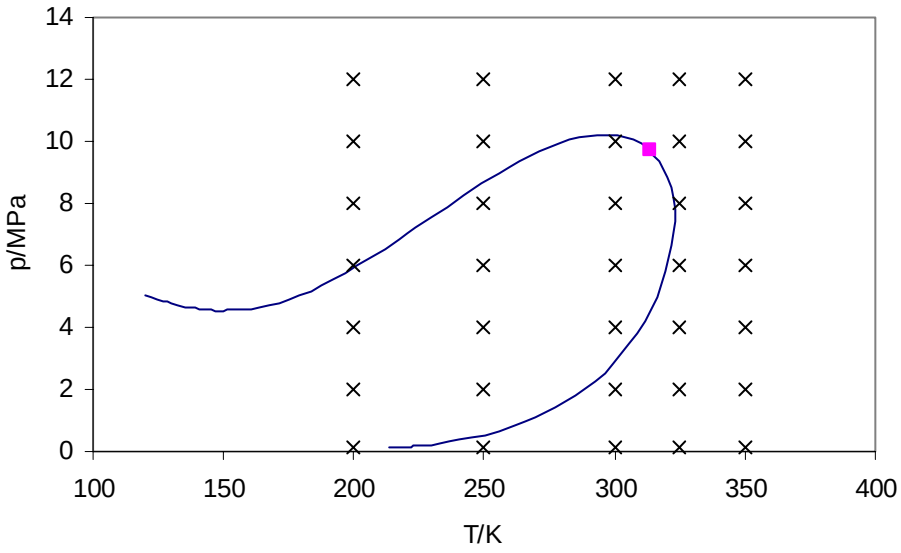

Figure 2.7. *Points flashed to test the robustness of the pT-flash.* ×*, flashed point;* ■*, critical point, z(H_2) = 0.02065, z(CH_4) = 0.54955*

Two bubble point temperatures at constant pressure are typical to hydrogen hydrocarbon mixture. In this example between 4.5 MPa and 5 MPa two bubble point temperatures at constant pressure can be found. The equation (2.66) at recovery routines is needed to fit the splines for this kind of phase envelope.

2.2.4 Binary ethane + limonene

The example where there are three dew point pressures at constant temperature is reported in Raeissi and Peters (2001). The Peng-Robinson equation of state without the use of the binary interaction parameter modelled the special shape of the dew point curve well. The measured and computed dew and bubble point curve were presented in Figure 2.8

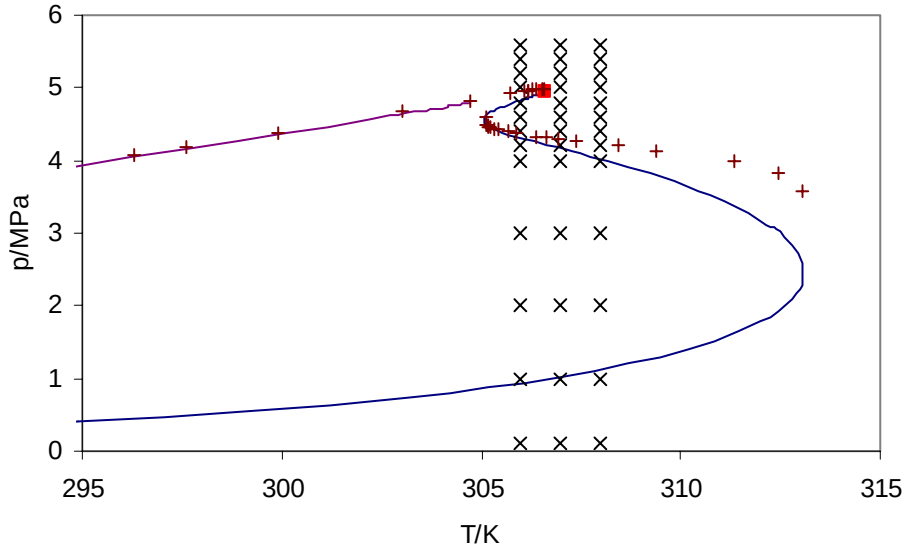

Figure 2.8. *Points flashed to test the robustness of the pT-flash.* ×, *flashed point;* ■, *critical point,* +, *measured by Raeissi and Peters (2001), z(C_2H_6) = 0.9993, z(limonene) = 0.0007*

The flash routine was tested in the vicinity of the critical point. It was found that the recovery routines were not needed. The equation (2.63) at recovery routines is needed to fit the splines for this kind of phase envelope.

2.3 Internal energy-volume flash

In papers [IX]-[X] the dynamics of pressure relief system of the processes operating near the critical point is studied. There are various studies in open literature where the safety aspects are studied with the aid of dynamic simulation. Salzano et al. (2003) studied the boiling liquid expanding vapour explosion (BLEVE) of the liquefied petroleum gas (LPG) tanks. Mahgerefteh et al. (1999, 2002) studied the blowdown of sylindrical vessels exposed to fire. Haque et al. (1992 a & b) studied the blowdown of pressure vessels. Chen et al. (1995 a & b) studied the two-phase blowdown from long sub-sea pipelines. The important aspect in these studies is the strength of material that is affected by the high temperature in case of fire or by the low temperature in case of blowdown. Saha and Carroll (1997) developed the internal energy-volume flash for dynamic filling of a vessel that contains only vapour and/or liquid. Pellegrini et al. (1997) studied the dynamics of condenser of the CSTR reactor and its protection with the safety valve. Cassata et al. (1993 a & b) studied the relief dynamics of the distillation column. The simulators presented in open literature are designed for different applications and comparison between them is difficult because the modelling assumptions are so different. The commercial program SuperChems of DIERS (The Design Institute for Emergency Relief Systems), Melhem (1997), is the computer program for simulation of emergency relief systems that probably contains the greatest number of models available. SuperChems is the successor of the Safire code developed by DIERS.

There was a need for dynamic simulation that takes into account the critical state of the fluid, the solid particles that may exist in the contents of the vessel due to the reaction, the net heat input as a function of time (look-up table), several inflows and outflows per vessel as a function of time (look-up table), the rupture disk or safety valve as a pressure relieving device and capable for design and rating of the simulated system.

Initially the total composition of the fluid, its temperature and pressure, the weight fraction of polymer to total mass of contents of the reactor and the mass of catalyst are known. The mass of fluid is computed from the density of fluid at given *T* and *p* and the volume the solid components do not occupy. This kind of initialisation allows the easy start of the simulation with *T* and *p*. The accuracy of the mass of fluid and the relative amounts of the vapour or liquid phase are dependent on the accuracy of the equation of state used. The total mass of material and internal energy is then

$$m_{TOT} = n\left((1-\beta)M_l + \beta M_v\right) + m_{POL} + m_{CAT} \tag{2.72}$$

$$U_{TOT} = n_{HC}\left((1-\beta)h_l + \beta h_v\right) + m_{POL}h_{POL} + m_{CAT}h_{CAT} - pV_{RCT} \tag{2.73}$$

where the total moles of fluid is defined by

$$n = \frac{V_{RCT} - V_{POL} - V_{CAT}}{(1-\beta)v_l + \beta v_v}$$

The individual components may react to form solid component. The balance for individual components, polymer and catalyst and their enthalpies are

$$\frac{dm_i}{dt} = \dot{m}_{i,in} - \dot{m}_{i,out} - r_i \tag{2.74}$$

$$\frac{dm_{POL}}{dt} = \dot{m}_{POL,in} - \dot{m}_{POL,out} + \sum_{i=1}^{C} r_i \tag{2.75}$$

$$\frac{dm_{CAT}}{dt} = \dot{m}_{CAT,in} - \dot{m}_{CAT,out} \tag{2.76}$$

$$\frac{dH}{dt} = \dot{n}_{in}h_{in} - \dot{n}_{out}h_{out} \tag{2.77}$$

$$\frac{dH_{POL}}{dt} = \dot{m}_{POL,in}h_{POL,in} - \dot{m}_{POL,out}h_{POL,out} \tag{2.78}$$

$$\frac{dH_{CAT}}{dt} = \dot{m}_{CAT,in}h_{CAT,in} - \dot{m}_{CAT,out}h_{CAT,out} \tag{2.79}$$

$$\frac{dU_{TOT}}{dt} = \frac{dH}{dt} + \frac{dH_{POL}}{dt} + \frac{dH_{CAT}}{dt} + \dot{Q}_{HE} + \dot{Q}_{FR} - \dot{Q}_{CL} + \dot{Q}_{MX} \tag{2.80}$$

The derivatives and the time step of integration are needed in calculation of the value of total mass and total internal energy one time step ahead.

$$m_{TOT,spec} = \sum_{i=1}^{C}\left(m_i^t + \frac{dm_i}{dt}\Delta t\right) + \left(m_{POL}^t + \frac{dm_{POL}}{dt}\Delta t\right) + \left(m_{CAT}^t + \frac{dm_{CAT}}{dt}\Delta t\right) \tag{2.81}$$

$$U_{TOT,spec} = U_{TOT}^t + \frac{dU_{TOT}}{dt}\Delta t \tag{2.82}$$

The two variables, temperature and pressure, were solved with the two variable Newton iteration. In this work during the iteration the maximum step size was limited to 5 K in temperature and to 100 kPa in pressure.

$$m_{TOT,spec} - m_{TOT}(T, p) = 0 \tag{2.83}$$

$$U_{TOT,spec} - U_{TOT}(T, p) = 0 \qquad (2.84)$$

Compared to paper [IX] some modifications and additions of the model equations were made; the kinetic energy term removed, DIERS model for two-phase, supercritical and gaseous flow added, API520 model for flashing flow added.

2.3.1 Example of dynamic simulation

The example originates from the paper [X] and its Table 2, "case b". The reactor described in the paper started to relieve at region of two phases and the relief continued to the gaseous region. In "case b" the model for the valve was the DIERS method and the vessel was very close to the critical point. This is presented in Figure 2.9.

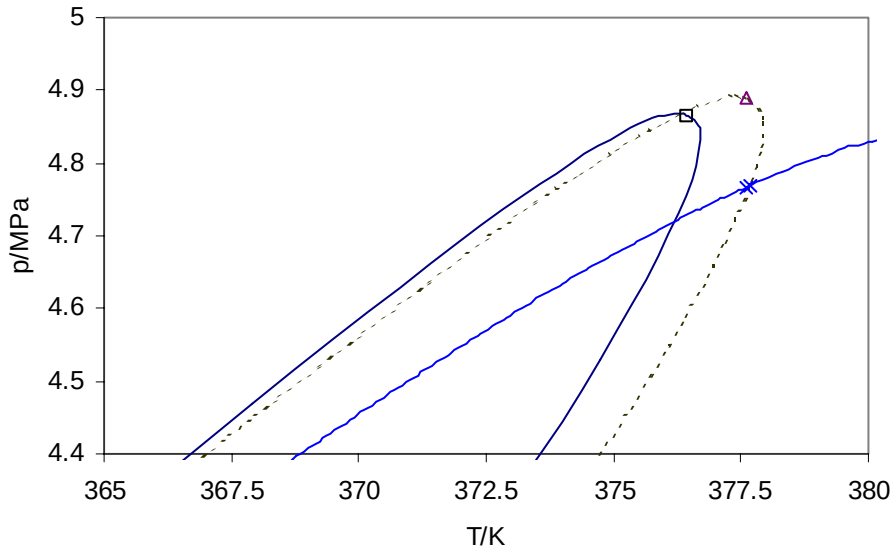

Figure 2.9 *Internal energy volume flash very near the phase boundary and the critical point. —, phase envelope at 0 seconds; - - - , phase envelope at 322 seconds; □, critical point at 0 seconds; △, critical point at 322 seconds; +, points of UV flash*
.

Two time steps of internal energy-volume flash (UV-flash) are presented in Table 2.4 and Table 2.5. The Table 2.4 shows the convergence of the last point inside the phase boundary. It takes 4 iterations for the UV-flash to converge and 40 successive substitution loops for pT-flash to converge.

Table 2.4. *Convergence of UV-flash at two phase region, refers to Figure 2.10*

UV, iter	pT, iter	T/K	p/Pa	BETA	diff m	diff U
0	40	377.5371623	4764331.973			
1	40	377.6081054	4766475.945	0.967325811	17.81866	-8498668
2	40	377.6082948	4766478.044	0.986765059	0.072013	-31840
3	40	377.6082947	4766478.044	0.986824199	-3.4E-05	14
4	40	377.6082947	4766478.044	0.986824177	0	0

The next point is outside the phase boundary as shown in Table 2.5

Table 2.5 *Convergence of UV-flash at single phase region, refers to Figure 2.10*

UV, iter	pT, iter	T/K	p/Pa	BETA	diff m	diff U
0	40	377.6082947	4766478.044			
1	41	377.6792139	4768599.516	0.984944877	17.80224	-8487646
2	41	377.6998816	4769677.354	1	1.018109	-641093
3	41	377.6998651	4769677.062	1	-0.004464	1831
4	41	377.6998651	4769677.062	1	6E-06	-2
5	41	377.6998651	4769677.062	1	0	0

The negative flash converged to $\beta = 1.01$ that indicates the gaseous phase. The limits for the vapour fraction at converged vapour fraction are $-1.82307 < \beta < 4.71468$.

2.4 Pressure-Enthalpy flash

Pressure enthalpy flash (pH-flash) is easily constructed if the pT-flash is robust. The structure is called "overiteration", where pT-flash is in the inner loop and enthalpy balance at the outer loop. Whitson and Michelsen (1989) used negative flash at the pressure-enthalpy flash because the enthalpy does not have continuous derivative at the phase boundary and thus the convergence is difficult.

The pT-flash I formulated identifies the phase vapour like, liquid like or vapour-liquid mixture. It uses the negative flash but does not allow the molar vapour fraction to exceed 1 or 0 in the routines where the thermodynamic properties, like the enthalpy, are calculated. The function to be solved is

$$f_h = H_{spec} - H \tag{2.85}$$

The Newton iteration of one variable starts easily to swing at the point where there is a rapid change of the derivative. The step size limitation in temperature does not help much. That's why the solving method is switched to the method of van Wijngaarden - Dekker – Brent presented by Press et al. (1994), immediately after the change in sign of function takes place. The method of van Wijngaarden - Dekker - Brent finds the root because it is a combination of root bracketing, bisection and inverse quadratic interpolation.

2.4.1 Example of pressure enthalpy flash

The previous example in Table 2.4 presents the state of the vessel. It was assumed that the discharge pipe does not cause any pressure drop. Then the DIERS model proposed that the stream is flashed adiabatically to 0.7 times the inlet pressure to solve a parameter needed in mass flux calculation. The adiabatic flash was iterated first with the one variable Newton iteration until the function changed its sign and continued with the method of van Wijngaarden - Dekker – Brent presented by Press et al. (1994).

During this project on dynamic simulation the initial guess for temperature of adiabatic flash is conveniently obtained from

$$p = a(T - T_{cf}) + p_{cf} \quad \text{where} \quad a = 0.122\ \text{MPa/K} \tag{2.86}$$

by solving the adiabatic initial temperature T_{cf} at p_{cf}, 0.7 times the inlet pressure. The convergence is presented in Table 2.6 and in Figure 2.10. The initial guess hits the gaseous phase, in this case the convergence was relatively fast.

Table 2.6. *Convergence of the enthalpy pressure flash*

One variable Newton	
T/K	fun = Hspec - H
365.943	-2462.31
360.943	-1091.95
355.943	2936.32
Root bracketing	
T/K	fun = Hspec - H
359.587	-147.841
359.385	2.16058
359.388	-1.79E-02
359.388	-2.14E-06

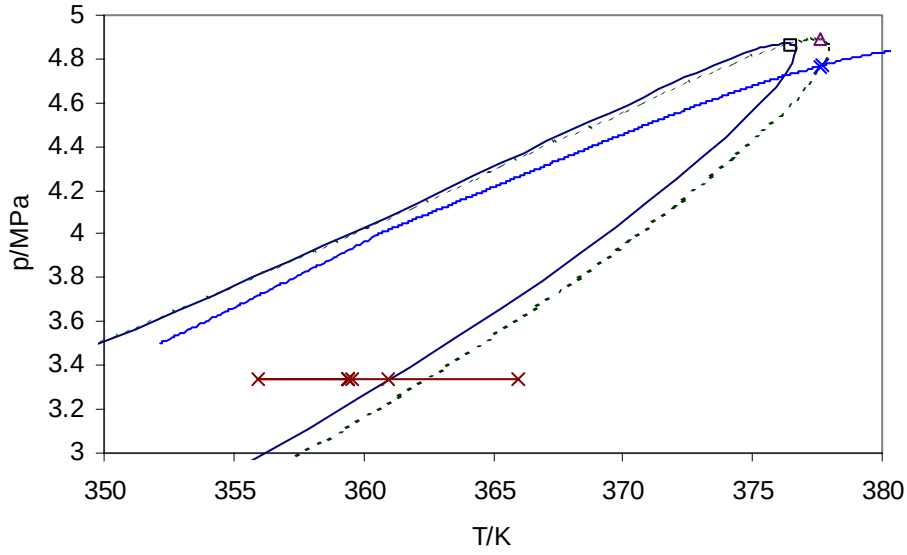

Figure 2.10. *Pressure enthalpy flash to 0.7 times the inlet pressure (DIERS model) and its convergence. —, phase envelope at 0 seconds; - - -, phase envelope at 322 seconds; □, critical point at 0 seconds; △, critical point at 322 seconds; ┼, points of pH flash .*

The pressure enthalpy flash is repeated thousands of times during a dynamic simulation. This kind of flash was found robust in this work.

3 Density modelling

3.1 Models for vapour phase only

At low pressure the vapour and gas density of a pure component and a mixture can be modelled relatively accurately. Even the ideal gas law gives sufficient accuracy. The virial equation of state as an expansion of the ideal gas law improves the accuracy of the vapour phase of a pure component or a mixture. According to Walas (1985), at subcritical temperature the virial equation of state can be applied up to density of saturated vapour, and at supercritical temperature it can be applied below 0.5 times the critical density. The drawback of ideal gas law and virial equation of state is that they can be applied to gas and vapour phase only.

3.2 Models for both vapour and liquid phase

More than one hundred years ago van der Waals proposed the celebrated equation to combine the liquid and vapour phase into the same model. Since then hundreds of modifications have been proposed to improve the pressure-volume-temperature behaviour and several reviews in the literature on this subject have been published, Valderrama (2003) and Ghosh (1999). There are three main research areas on equation of state: to improve the temperature dependence of the attraction term especially for polar fluids, to improve volumetric accuracy especially for the dense phase, and to improve mixing rules for the mixtures.

One of the ways to improve the volumetric accuracy is increasing the number of parameters of cubic equation of state, and the volume translation belongs to the above method. The following papers propose a volume translation: Soave (1984), Mathias et al. (1989), Chou and Prausnitz (1997), Ji and Lempe (1997, 1999), Zabylon and Brignole (1997), Tsai and Chen (1998) and Monnery (1998). The danger of the temperature-dependent volume translations is the crossing isotherms at high densities, Pfohl (1999). He also warned to apply the temperature-dependent volume translations outside the space where their constants have been fitted.

The volumetric accuracy is improved also by increasing the degree of volume roots of the equation of state, usually from cubic to quartic. Two examples of quartic equations of state are Shah et al. (1996) and Zhi et al. (2001).

There are equations of state where the degree of volume roots is higher than four and they have a great number of parameters. Span et al. (2001) divided these into the reference and the technical equations of state. The purpose of the reference equation of state is to describe all experimentally available measurements for a certain fluid within their experimental accuracy. The reference equations of state also have extrapolative capability and numerical stability at extreme temperature and pressure. Span et al. (2001) tabulated recommended reference equations of state for 30 pure components. The technical equations of state are developed based on less accurate measurements and smaller sets of measurements, Span et al. (2001). The risk of

technical equations of state is in the extrapolation of model outside the range for which it is developed.

3.3 Models for liquid phase only

For the saturated liquid density of pure component there are component-specific and generalised correlations. The correlations of Daubert and Danner (1989) and Yaws (1999) are examples of component-specific correlations. The mathematical equation is the same, but the coefficients are optimised against the measurement of each component. The generalised correlation estimates the density based on the critical properties of the component, for example the Rackett (1970) correlation, and does not need component-specific parameters. The density of compressed liquid is correlated usually with the aid of saturated liquid density and a special term that takes into account the compression, for example Chang and Zhao (1990) .

3.4 Extension of the temperature range of Aalto-Keskinen (1999) model

The model of Aalto and Keskinen (1999) gives the density of liquid mixture accurately but its drawback is the limited temperature range. This is due to a big deviation of the pseudo-critical point compared to the measured critical point. Usually the pseudo-critical point is lower than the measured critical point. Furthermore, the pseudo-bubble point pressure is usually lower than the measured bubble point pressure.

Target is to extend and make a more consistent model by using cubic equation of state to provide more realistic critical properties and bubble point pressure [XI]. The location of the critical point of the mixture is more realistic with the equation of state compared to pseudo-critical properties. In addition, the bubble point pressure is more realistic with the equation of state than vapour pressure correlation.

The study [XI] to extend the temperature range of the Aalto and Keskinen (1999) model shows that using rigorous thermodynamics extends the range but at the expense of the accuracy. However, the accuracy of the extended model is still better than the accuracy of the SRK equation of state. This can be seen in Table 3.1 and Table 3.2 where the density computed from the SRK is compared with the extended model “alternative 4”.

Table 3.1 *Accuracy of density predictions for binary systems*

methane+ethane		NOP	%-rel.error	abs %-rel.error
	alternative 1	231	-0.43	0.44
	alternative 2	231	-0.54	0.55
	alternative 3	248	1.16	1.22
	alternative 4	248	1.02	1.14
	SRK	248	-2.53	2.53
methane+propane		NOP	%-rel.error	abs %-rel.error
	alternative 1	150	-0.43	0.56
	alternative 2	150	-1.84	1.86
	alternative 3	215	2.76	3.30
	alternative 4	215	1.74	2.57
	SRK	215	-4.48	4.48
methane+butane		NOP	%-rel.error	abs %-rel.error
	alternative 1	68	0.69	0.89
	alternative 2	67	-1.53	1.59
	alternative 3	109	5.36	5.50
	alternative 4	105	2.77	3.12
	SRK	105	-4.99	4.99
methane+pentane		NOP	%-rel.error	abs %-rel.error
	alternative 1	153	0.28	0.40
	alternative 2	153	-1.96	1.96
	alternative 3	218	6.15	6.15
	alternative 4	218	4.66	4.66
	SRK	218	-6.89	6.89
methane+cyclohexane		NOP	%-rel.error	abs %-rel.error
	alternative 1	452	0.77	0.80
	alternative 2	409	-1.43	1.53
	alternative 3	536	5.38	5.54
	alternative 4	441	3.56	3.56
	SRK	441	-5.04	5.04
methane+decane		NOP	%-rel.error	abs %-rel.error
	alternative 1	432	0.35	0.70
	alternative 2	432	-1.98	2.01
	alternative 3	483	5.26	5.28
	alternative 4	483	4.32	4.37
	SRK	476	-14.23	14.23
methane+decane		NOP	%-rel.error	abs %-rel.error
	alternative 1	220	1.30	1.33
	alternative 2	220	-3.06	3.07
	alternative 3	400	9.91	9.91
	alternative 4	363	8.00	8.00
	SRK	363	-12.43	12.43
methane+decane		NOP	%-rel.error	abs %-rel.error
	alternative 1	176	-0.18	0.35
	alternative 2	176	-2.75	2.75
	alternative 3	176	4.60	4.60
	alternative 4	176	3.93	3.93
	SRK	176	-15.63	15.63

Table 3.2 *Accuracy of density predictions for ternary systems*

methane+propane+decane	NOP	%-rel.error	abs %-rel.error
alternative 1	115	0.93	0.96
alternative 2	115	-1.07	1.42
alternative 3	179	8.68	8.68
alternative 4	179	7.59	7.59
SRK	179	-11.24	11.24

methane+butane+decane	NOP	%-rel.error	abs %-rel.error
alternative 1	57	0.15	0.59
alternative 2	57	-3.83	3.84
alternative 3	154	10.12	10.16
alternative 4	152	8.23	8.36
SRK	152	-9.47	9.47

methane+butane+decane	NOP	%-rel.error	abs %-rel.error
alternative 1	353	0.77	0.97
alternative 2	353	-2.34	2.49
alternative 3	546	8.79	8.80
alternative 4	532	7.18	7.22
SRK	532	-10.21	10.21

Conclusion

Two apparatus for the measurement of vapour liquid equilibrium were built. The recirculation still allowed isothermal and isobaric measurements at atmospheric pressure or at vacuum. The total pressure apparatus allowed isothermal measurement, the maximum pressure was 20 bar. The automation for the total pressure apparatus was built. Several hydrocarbon alcohol systems were measured. The systems had importance in developing processes for gasoline additives. The non-ideality of the liquid phase was correlated with activity coefficient models and of the vapour phase with cubic equation of state. The optimisation of model parameters was discussed.

The dynamic simulator for the emergency relief was developed. The special importance was the robustness of the flash routines near the vapour liquid critical point of the system. The convergence of the flash routine is very difficult near the critical point causing the routine in some cases not to converge. Special routines to recover from the fail of flash were developed. These allowed the determination of the phase and the continuation of the simulation. The simulator had importance in design of safety valves, dump tanks and flare systems.

The temperature range of a model for compressed liquid density of mixture was extended. The rigorous bubble point pressure and the critical point computed from the cubic equation of state were more consistent with the experimental data than the pseudo bubble point and pseudo critical point of the original model. The application range of the compressed liquid density model was extended at the expense of accuracy but the extended model was better than a cubic equation of state.

References

Aalto, M.M. & Keskinen, K.I., (1999), Liquid Densities and High Pressure, *Fluid Phase Equilib.* **166,** 183-205.

Adachi, Y., Lu, B.C.-L. & Sugie, H., (1983), A Four-Parameter Equation of State, *Fluid Phase Equilib.* **11,** 29-48.

Amman, M.N. & Renon, H., (1987), The Isothermal Flash Problem: New Methods for Phase Split Calculations, *AIChE J*. **33**, 926-939.

Assilineau, L. & Renon, H., (1970), Extension de l'équation NRTL pour la representation de l'énsemble des données d'équilibre binaire, liquide-vapeur et liquide-liquide, Chem. Eng. Sci. **25**, 1211-1223.

Barker, J.A., (1953), Determination of Activity Coefficients from Total Pressure Measurements, *Austral. J. Chem*. **6**, 207-210.

Bünz, A.P., Dohrn, R., Prausnitz, J.M., (1991), Three-Phase Flash Calculations for Multicomponent Systems, *Comp. Chem. Engng.*, **15**(1), 47-51.

Cassata, J.R., Dasgupta, S. & Gandhi, S.L., (1993), Modeling of Tower Relief Dynamics, Part 1, Hydrocarbon Processing, **72**(10), 71-76.

Cassata, J.R., Dasgupta, S. & Gandhi, S.L., (1993), Modeling of Tower Relief Dynamics, Part 2, Hydrocarbon Processing, **72**(11), 69-74.

Chang, C.-H. & Zhao, X. M., (1990), A New Generalised Equation of Predicting Volumes of the Compressed Liquids, *Fluid Phase Equilib.*, **58**, 231-238.

Chen, J.R., Richardson, S.M. & Saville, G., (1992), Modelling of Two-phase Blowdown from Pipelines- I. A hyperbolic Model Based in Variational Principles, *Chem. Engng. Sci*. **50**(4), 695-713.

Chen, J.R., Richardson, S.M. & Saville, G., (1992), Modelling of Two-phase Blowdown from Pipelines- II. A Simplified Numerical Method for Multi-Component Mixtures, *Chem. Engng. Sci*. **50**(13), 2173-2187.

Chou, G.F. & Prausnitz, J.M., (1989), A Phenomenological Correction to an Equation of State for the Critical Region, *AIChE Journal* **35**, 1487-1496.

Christensen, C., Gmehling, J., Rasmussen, P. & Weidlich, U., (1984), *Heats of Mixing Data Collection, Binary and Multicomponent Systems, Dechema Chemistry Data Series*, Vol. III, Part 2.

Christensen, J.J., Rowley, R.L. & Izatt, R.M., (1988), *Handbook of Heats of Mixing, Supplementary volume*, John Wiley & Sons, New York.

Constantinides, A., & Mostoufi, N., (1999), *Numerical Methods for Chemical Engineers with MATLAB Applications*, Prentice Hall, New Jersey.

Coward, I., Gale S.E., & Webb, D.R., (1978), Process Engineering Calculations with Equations of State, *Trans IchemE*, **56**, 19-27.

Cutlip, M.B., & Shacham, M., (1999), *Problem Solving in Chemical Engineering with Numerical Methods*, Prentice Hall, New Jersey.

Daubert, T., E. & Danner, R., P. (1989), *Physical and Thermodynamic Properties of Pure Chemicals: Data Compilation*; Hemisphere: New York.

Davalos, J., Anderson, W.R., Phelps, R.E. & Kidnay, A.J., (1976), Liquid-Vapor Equilibria at 250.00 K for Systems Containing Methane, Ethane, and Carbon Dioxide, *J. Chem.Eng Data*, **21**, 81-84.

Davidon, W. C., (1975), Optimally Conditioned Optimization Algorithms without Line Searches, *Math. Programming* **9**, 1-30.

Fredenslund, Aa., Gmehling, J. & Rasmussen, P., (1977), *Vapor-Liquid Equilibria Using UNIFAC*, Elsevier, Amsterdam, 1977.

Gautam, R. & Seider, W.D., (1979), Computation of Phase and Chemical Equilibrium: Part I, Local and Constrained Minima in Gibbs Free Energy, *AIChE J*. **25**, 911-1006.

Gibbs, R.E. & van Ness, H.C., (1972), Vapor-Liquid Equilibria from Total-Pressure Measurements. A New Apparatus, *Ind. Eng. Chem. Fundam*, **11**(3), 410-413

Gillespie, D.T.C., (1946), Vapor-Liquid Equilibrium Still for Miscible Liquids, *Ind. Eng. Chem., Anal. Ed.*, **18**(9), 575-577.

Ghosh, P., (1999), Review: Prediction of Vapor-Liquid Equilibria Using Peng-Robinson and Soave-Redlich-Kwong Equations of State, *Chem. Eng. Technol.*, **22**(5), 379-399

Gmehling, J. & Onken, U., (1977), *Vapor-Liquid Equilibrium Data Collection; DECHEMA Chemistry Data Series*, Vol 1, Part 1; DECHEMA: Frankfurt/Main.

Gossett, R., Heyen. G. & Kalitventzeff, B., (1986), An Efficient Algorithm to Solve Cubic Equations of State, *Fluid Phase Equilib*. **23**, 51-64.

Gundersen, T., (1982), Numerical Aspects of the Implementation of Cubic Equations of State in Flash Calculation Routines, *Comp. Chem. Engng.*, **6**(3), 245-255

Hague, M.A., Richardson S.M. & Saville, G., (1992), Blowdown of Pressure Vessels, I. Computer Code, *Trans IChemE*, **70**, part B, 3-9.

Hague, M.A., Richardson S.M., Saville, G., Chamberlain, G. & Shirvill, L., (1992), Blowdown of Pressure Vessels, II. Experimental Validation of Computer Model and Case Studies, *Trans IChemE*, **70**, part B, 10-9.

Hankinson, R.W. & Thomson, G.H., (1979), A New Correlation for Saturated Densities of Liquids and Their Mixtures, *AIChE J*. **25**, 653-663.

Heidemann, R.A. & Khalil, A.M., (1980), The Calculation of Critical Points, *AIChE J.* **26**, 769-779.

Ji, W.-R. & Lempe, D.A., (1997), Density Improvement of the SRK Equation of State, *Fluid Phase Equilib.* **130,** 49-63.

Ji, W.-R. & Lempe, D.A., (1999), Erratum to "Density Improvement of the SRK Equation of State", *Fluid Phase Equilib.* **155,** 339.

Knapp, H., Zeck, S. & Langhorst, R., (1989), *Vapor-Liquid Equilibria for Mixtures of Low Boiling Substances, Ternary Systems, Dechema Chemistry Data Series*, Vol VI, Part 3, p. 743-754

Kojima, K.; Moon, H. & Ochi, K., (1990), Thermodynamic Consistency Test of Vapor-Liquid Equilibrium Data, *Fluid Phase Equilib.* **56**, 269-284.

Kolbe, B., & Gmehling, J., (1985), Thermodynamic Properties of Ethanol + Water. I. Vapour-Liquid Equilibria Measurements from 90 to 150 °C by Static Method, *Fluid Phase Equilib.* ***23***, 213-226.

Larsen, B.L., Rasmussen, P. & Fredenslund, Aa., (1987), A Modified UNIFAC Group Contribution Model for the Prediction of Phase Equilibria and Heat of Mixing, *Ind. Eng. Chem. Res*, **26**, 2274.

Lucia, A. & Taylor, R., (1992), Complex Iterative Solutions to Process Model Equations ?, European Symposium on Computer Aided Process Engineering, *Comp. Chem. Engng.*, **16**, S387-S394.

Mahgerefteh, H. & Wong, S.M.A., (1999), A Numerical Blowdown Simulation Incorporating Cubic Equations of State, *Comp. Chem. Engng.*, **23**(9), 1309-1317.

Mahgerefteh, H., Falope, G.B.O. & Oke, A.O., (2002), Modeling Blowdown of Cylindrical Vessels Under Fire Attack, *AIChE J*., **48**, 401-410.

Mathias, P.M., Naheiri, T. & Oh, E.M., (1989), A Density Correction for the Peng-Robinson Equation of State, *Fluid Phase Equilib.* **47**, 77-87.

Mentzer, R.A., Greenkorn, R.A. & Chao, K.C., (1982), Bubble Pressures and Vapour-Liquid Equilibria for Four Binary Hydrocarbon Mixtures, *J. Chem. Thermod.* **14**, 817-830.

Melhem, G.A. & Fischer, H.G., (1997), An Overview of SuperChems for DIERS: A Program for Emergency Relief System and Effluent Handling Designs, *Proc Safety Progress.*, **16**(3), 185-197.

Michelsen, M.L., (1980), Calculation of Phase Envelopes and Critical Points for Multicomponent Mixtures, *Fluid Phase Equilib.* **4**, 1-10.

Michelsen, M.L., (1982 a), The Isothermal Flash Problem. Part I. Stability, *Fluid Phase Equilib.* **9**, 1-19.

Michelsen, M.L., (1982 b), The Isothermal Flash Problem. Part II. Phase Split Calculation, *Fluid Phase Equilib.* **9**, 21-40.

Michelsen, M.L., (1994), A Simple Method for Calculation of Approximate Phase Boundaries, *Fluid Phase Equilib.* **98**, 1-11.

Mixon, F.O., Gumowski, B. & Carpenter, B.H., (1965), Computation of Vapor-Liquid Equilibrium Data from Solution Vapor Pressure Measurements, *Ind. Eng. Chem., Fundam.,* **4**, 455-459.

Mollerup, J.M. & Michelsen, M.L., (1996), *Course Notes for Ph.D.-course August 1996*, Danmarks Tekniske Universitet, Lyngby.

Monnery, W.D., Svrcek, W.Y. & Satyro, M.A., (1998), Gaussian-like Volume Shifts for the Peng-Robinson Equation of State, *Ind. Eng. Chem. Res.* **37**, 1663-1672.

Monroy-Loperena, R., (2001), Efficient, Robust, and Reliable Single-Stage Vapor-Liquid Flash Calculations, *Ind. Eng. Chem. Res*. **40**, 3792-3800.

Munjan, S., Muthu, O., Khurma, J.R. & Smith, B.D., (1983), Reduction of Total-Pressure Vapor-Liquid Equilibrium Data. Comparison of Data Reduction Methods, Reliability of γ_i^{∞} Values, and Effect of Equation of the Equation of State Assumed, *Fluid Phase Equilibria*, **12**, 29-50.

Nelson, P.A., (1987), Rapid Phase Determination in Multiple-Phase Flash Equilibrium Calculations, *Comp. Chem. Engng.*, **11**(6), 581-591.

Nichita, D.V., Gomez, S., & Luna, E, (2002), Multiphase Equilibria Calculation by Direct Minimization of Gibbs Free Energy with a Global Optimization Method, *Comp. Chem. Engng.*, **26**(12), p. 1703-1724.

Nicolaides, G.L. & Eckert, C.A., (1978), Optimal Representation of Binary Liquid Mixture Nonidealities, *Ind. Eng. Chem. Fundam*. **17**, 331-340.

Ohanomah, M.O. & Thompson, D.W., (1984), Computation of Multicomponent Phase Equilibria- Part I. Vapour-Liquid Equilibria, *Comp. Chem. Engng.*, **8**(3/4), 147-156.

Othmer, D.F., (1928), Composition of Vapors from Boiling Binary Solutions, *Ind. Eng. Chem.*, **20**(7), 743-746.

Pellegrini, L., Biardi. G., Caldi M.L. & Monteleone, M.R., (1997), Checking Safety Relief Valve Design by Dynamic Simulation, *Ind. Eng. Chem. Res.*, **36**, 3075-3080.

Peng, D.-Y. & Robinson, D.B., (1976), A New Two-Constant Equation of State, *Ind. Eng. Chem., Fundam.* **15**, 59-64.

Perry, R.H., & Green, D.W., (1997), *Perry's Chemical Engineers' Handbook*, 7th ed. McGraw-Hill, New York.

Pfohl, O., (1999), Letter to the editor: Evaluation of an Improved Volume Translation for the Prediction of Hydrocarbon Volumetric Properties, *Fluid Phase Equilib.* **163**, 157-159.

Plank, C.A., Olson, J.D., Null, H.R., Muthu, L. & Smith, B.D., (1981), Reduction of Total-Pressure Vapor-Liquid Equilibrium Data. Common Pitfalls Encountered, *Fluid Phase Equilib.* **6**, 39-59.

Poling, B.E., Prausnitz, J.M. & O'Connell, J.P., (2001), *The Properties of Gases and Liquids*, 5th ed., McGraw-Hill, New York.

Press, W.H., Teukolsky, S.A., Vetterling, W.T. & Flannery, B.P., (1994), *Numerical Recipes in Fortran, The Art of Scientific Computing*, 2nd edition, Cambridge University Press, Cambridge.

Raal, J.D. & Mühlbauer, A.L., (1998), *Phase Equilibria, Measurement and Computation*, Taylor and Francis, USA.

Rachford, H.H. Jr. & Rice, J.D., (1952 Oct), Procedure for Use of Electrical Digital Computers in Calculating Flash Vaporization Hydrocarbon Equilibrium, *J. Petrol. Technology*, **4**(10), sec. 1, p. 19 and sec. 2, p. 3.

Racket, H.G., (1970), Equation of State for Saturated Liquids, *J. Chem. Eng. Data*, **15**, 514-517

Raeissi, S. & Peters, C.J., (2001), On the Phenomenon of Double Retrograde Vaporisation: Multi-dew Point Behavior in the Binary System Ethane + Limonene, *Fluid Phase Equilib.* **191**, 33-40.

Rarey, J.R. & Gmehling, J., (1993), Computer-Operated Differential Static Apparatus for the Measurement of Vapor-Liquid Equilibrium Data. *Fluid Phase Equilib.* **83**, 279-287.

Renon, H. & Prausnitz, J.M., (1968), Local Composition in Thermodynamic Excess Functions for Liquid Mixtures, *AIChE J.* **14**, 135-144.

Roche, M., & Li, W. X., (July 1987), A Note on Real Time Parametric Cubic Segment Curve Generation, *Intelligent Instruments & Computers*, 168-174.

Rose, L.M., (1981), *Chemical Reactor Design in Practice*, Elsevier, Amsterdam.

Ronc, M. & Ratcliff G.R., (1976), Measurement of Vapor-Liquid Equilibria Using a Semi-Continuous Total Pressure Static Equilibrium Still, *Can. J. Chem. Eng.*, **54**, 327-332.

Saha, S. & Carroll, J.J., (1997), The Isoenergetic-Isochoric Flash, *Fluid Phase Equilib.* **138**, 23-41

Salzano, E., Picozzi, B., Vaccaro, S. & Ciambelli, P., (2003), Hazards of Pressurized Tanks Involved in Fires, *Ind. Engng. Chem. Res.*, **42**, 1804-1812

Shacham, M. & Brauner, N., (1997), Minimizing the Effects of Collinearity in Polynomial Regression, *Ind. Eng. Chem. Res*. **36**, 4405-4412.

Shah, V.M., Lin, Y.-L., Bienkowski, P.R. & Cochran, H.D., (1996), A Generalized Quartic Equation of State, *Fluid Phase Equilib.* **116**, 87-93.

Skjold-Jørgensen, S., Rasmussen, P. & Fredenslund, AA., (1980), On the Temperature Dependence of the UNIQUAC/UNIFAC Models, *Chem. Eng. Sci.* **35**, 2389-2403.

Smith, J.M., Van Ness, H.C. & Abbott, M.M., (1996), *Introduction to Chemical Engineering Thermodynamics*, 5th edition, McGraw-Hill, Singapore.

Soave, G., (1972), Equilibrium Constants from a Modified Redlich-Kwong Equation of State, *Chem. Eng. Sci.* **27**, 1197-1203.

Soave, G., (1984), Improvement on the van der Waals Equation of State, *Chem. Eng. Sci.* **39**, 357-369.

Sofyan, Y., Ghajar, A.J. & Gasem, K.A.M, (2003), Multiphase Equilibrium Calculations Using Minimization Techniques, *Ind. Eng. Chem. Res*. **42**, 3786-3801.

Span, R., Wagner, W., Lemmon, E.W. & Jacobsen, R.T., (2001), Multiparameter Equations of State – Recent Trends and Future Challenges, *Fluid Phase Equilib.* **183-184**, 1-20.

Spencer, C.F. & Danner, R.P., (1972), Improved Equation for Prediction of Saturated Liquid Density, *J. Chem. Eng. Data*, **17**, 236-241.

Sun, A.M. & Seider, W.D., (1995), Homotopy-Continuation Method for Stability Analysis in the Global Minimization of the Gibbs Free Energy, *Fluid Phase Equilib.* **103**, 213-249.

Trebble, M.A., (1989), A Preliminary Evaluation of Two and Three Phase Flash Initiation Procedures, *Fluid Phase Equilib*. **53**, 113-122.

Tsai, J.-C. & Chen, Y.-P., (1998), Application of a Volume-Translated Peng-Robinson Equation of State on Vapor-Liquid Equilibrium Calculations, *Fluid Phase Equilib.* **145**, 193-215.

Uusi-Kyyny, P., Tarkiainen, V., Kim, Y., Ketola, R.A. & Aittamaa, J., (2003), Vapor Liquid Equilibrium for Ethanol + 2,4,4-Trimethyl-1-pentene and 2-Propanol + 2,4,4-Trimethyl-1-pentene at 101 kPa, *J. Chem.Eng Data*, **48**, 280-285.

Valderrama, J.O., (2003), The State of the Cubic Equations of State, *Ind. Eng. Chem. Res*., **42**, 1603-1618.

Walas, S.M., (1985), *Phase Equilibria in Chemical Engineering*, Butterworth Publishers, Stoneham.

Weidlich, U. & Gmehling, J., (1987), A Modified UNIFAC model. 1. Prediction of VLE, hE, and γ^{∞}, *Ind. Eng. Chem. Res*., **26**, 1372-1381.

Whitson, C.H. & Michelsen, M.L., (1989), The Negative Flash, *Fluid Phase Equilib.* **53**, 51-71.

Wilson, G.M., (1964), Vapor-Liquid Equilibrium XI: A New Expression for the Excess Free Energy of Mixing. *J. Am. Chem. Soc*., **86**, 127-130.

Wilson, G.A., (1968), Modified Redlich-Kwong Equation of state. Application to General Physical Data Calculations, *Paper 15c Presented at the Americal Institute of Chemical Engineers National Meeting*, Claveland.

Yaws, C.L., (1999), *Chemical Properties Handbook*, McGraw-Hill, New York.

Yerazunis, S., Plowright, J.D. & Smola, F.M., (1964), Vapor-Liquid Equilibrium Determination by a New Apparatus. *AIChE J*., **10**, 660-665.

Zabylon, M.S. & Brignole, E.A., (1997), On Volume Translations in Equations of State, *Fluid Phase Equilib.* **140**, 87-95.

Zhi, Y., Meiren, S., Jun, S. & Lee, H., (2001), A New Quartic Equation of State, *Fluid Phase Equilib.* **187-188**, 275-298.

Ziervogel, R. G. & Poling, B.E., (1983), A Simple Method for Constructing Phase Envelopes for Multicomponent Mixtures, *Fluid Phase Equilib.* **11**, 127-135